AD-A063 852   DUKE UNIV MEDICAL CENTER DURHAM N C DEPT OF OPHTHALMOLOGY   F/G 20/5
ELECTROPHYSIOLOGICAL DETERMINATION OF RETINAL SENSITIVITY TO CO--ETC(U)
SEP 78   M L WOLBARSHT   F41609-76-C-0020
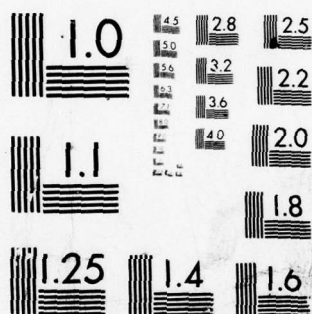UNCLASSIFIED   SAM-TR-78-9   NL

| OF |

AD
A063 852

END
DATE
FILMED

3--79
DDC

1.0

4.5
5.0
5.6
6.3

2.8

2.5

3.2

2.2

3.6

1.1

4.0

2.0

1.8

1.25

1.4

1.6

MICROCOPY RESOLUTION TEST CHART
NATIONAL BUREAU OF STANDARDS-1963-A

(18) Report SAM-TR-78-9   (19)   LEVEL

AD A063852

(6)

ELECTROPHYSIOLOGICAL DETERMINATION OF RETINAL SENSITIVITY TO COLOR AFTER INTENSE MONOCHROMATIC LIGHT ADAPTATION.

(10) Myron L. Wolbarsht, Ph.D.

Department of Ophthalmology
Duke University Medical Center
Durham, North Carolina 27710

DDC
RECEIVED
JAN 29 1979
A

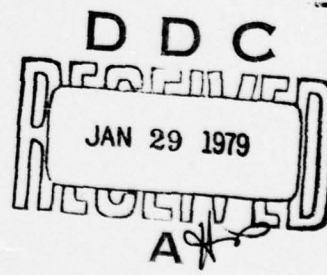Approved for public release; distribution unlimited.

Prepared for

USAF SCHOOL OF AEROSPACE MEDICINE
Aerospace Medical Division (AFSC)
Brooks Air Force Base, Texas 78235
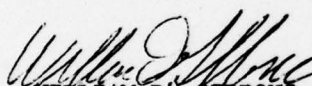
JOB

407 375

79 01 24 010

NOTICES

This final report was submitted by the Department of Ophthalmology, Duke University Medical Center, Durham, North Carolina 27710, under contract F41609-76-C-0020, job order 7757-02-57, with the USAF School of Aerospace Medicine, Aerospace Medical Division, AFSC, Brooks Air Force Base, Texas. Lieutenant Colonel William D. Gibbons (SAM/RZL) was the Laboratory Project Scientist-in-Charge.

When U.S. Government drawings, specifications, or other data are used for any purpose other than a definitely related Government procurement operation, the Government thereby incurs no responsibility nor any obligation whatsoever; and the fact that the Government may have formulated, furnished, or in any way supplied the said drawings, specifications, or other data is not to be regarded by implication or otherwise, as in any manner licensing the holder or any other person or corporation, or conveying any rights or permission to manufacture, use, or sell any patented invention that may in any way be related thereto.
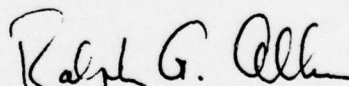
The animals involved in this study were procured, maintained, and used in accordance with the Animal Welfare Act of 1970 and the "Guide for the Care and Use of Laboratory Animals" prepared by the Institute of Laboratory Animal Resources - National Research Council.

This report has been reviewed by the Information Office (OI) and is releasable to the National Technical Information Service (NTIS). At NTIS, it will be available to the general public, including foreign nations.

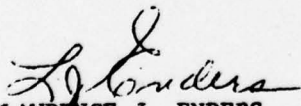This technical report has been reviewed and is approved for publication.

WILLIAM D. GIBBONS, Lt Col, USAF, BSC   RALPH G. ALLEN, Ph.D.
Project Scientist-in-Charge   Supervisor

LAWRENCE J. ENDERS
Colonel, USAF, MC
Commander

REPORT DOCUMENTATION PAGE		READ INSTRUCTIONS BEFORE COMPLETING FORM
1. REPORT NUMBER SAM-TR-78-9	2. GOVT ACCESSION NO.	3. RECIPIENT'S CATALOG NUMBER
4. TITLE *(and Subtitle)* ELECTROPHYSIOLOGICAL DETERMINATION OF RETINAL SENSITIVITY TO COLOR AFTER INTENSE MONOCHROMATIC LIGHT ADAPTATION		5. TYPE OF REPORT & PERIOD COVERED Final Report Dec. 1975 – Jan. 1977
		6. PERFORMING ORG. REPORT NUMBER
7. AUTHOR(s) Myron L. Wolbarsht, Ph.D.		8. CONTRACT OR GRANT NUMBER(s) F41609-76-C-0020
9. PERFORMING ORGANIZATION NAME AND ADDRESS Department of Ophthalmology Duke University Medical Center Durham, North Carolina 27710		10. PROGRAM ELEMENT, PROJECT, TASK AREA & WORK UNIT NUMBERS 62202F 7757-02-57
11. CONTROLLING OFFICE NAME AND ADDRESS USAF School of Aerospace Medicine (RZL) Aerospace Medical Division (AFSC) Brooks Air Force Base, Texas 78235		12. REPORT DATE September 1978
		13. NUMBER OF PAGES 49
14. MONITORING AGENCY NAME & ADDRESS*(if different from Controlling Office)*		15. SECURITY CLASS. *(of this report)* Unclassified
		15a. DECLASSIFICATION/DOWNGRADING SCHEDULE

16. DISTRIBUTION STATEMENT *(of this Report)*

Approved for public release; distribution unlimited.

17. DISTRIBUTION STATEMENT *(of the abstract entered in Block 20, if different from Report)*

18. SUPPLEMENTARY NOTES

19. KEY WORDS *(Continue on reverse side if necessary and identify by block number)*

laser; intense light sources; retinal ganglion cells; cat vision; color reception; electrophysiology; light adaptation; receptive fields; retina

20. ABSTRACT *(Continue on reverse side if necessary and identify by block number)*

Techniques were developed to record retinal ganglion-cell responses. Categories of cell types in the cat retina were established in which X, Y, and W cell types were found with both cones and rods. The cones were connected in combinations selected from three groups whose λ_{max} were 450, 500, and 555 nm. The receptive field organization showed center-surround characteristics interaction, including antagonism between cone types. Strong light adaptation showed independence of each cone group from any other in their influence

DD $_{1\ JAN\ 73}^{FORM}$ **1473** EDITION OF 1 NOV 65 IS OBSOLETE UNCLASSIFIED

79 01 24 010

20. ABSTRACT (continued)

upon the ganglion cells, which was confirmed by the separate recovery of sensitivity by each group. Both the loss and recovery of sensitivity in various parts of the receptive field were demonstrated. No special deleterious effects of strong light adaptation on the 450 λ_{max} cone were observed. Good stability of recording techniques was achieved with single cells maintained 10 hours or more. The central portion of the retina was studied intensively, demonstrating the feasibility of recording from the macular or foveal region in rhesus monkeys.

TABLE OF CONTENTS

LIST OF FIGURES

1

LIST OF TABLES

2

ELECTROPHYSIOLOGICAL DETERMINATION OF RETINAL SENSITIVITY
AFTER INTENSE MONOCHROMATIC LIGHT ADAPTATION

INTRODUCTION

The overall purpose of this research was to investigate a method for demonstrating changes in retinal ganglion-cell function after high-intensity radiation such as from a laser or other monochromatic source in the visible region. These experiments were designed to facilitate understanding functional retinal changes required to produce flash-blindness or permanent damage in human eyes, especially in the macular region which is so important in safety measures. Recordings were made from selected and well-characterized ganglion cells in animal retinas. Changes in receptive-field sensitivities were detected as a result of exposure to high-intensity monochromatic or broad-band light in part or all of the field. The time course of sensitivity recovery was also plotted. These results were then correlated with physiological and psychophysical data already known from other animal and human studies. The specific objective of this study was to delineate means by which ganglion cell responses could be used to evaluate color vision and visual-field loss after laser exposure of the monkey retina. Rabbit and cat retinas were used in developing the experimental techniques required for this evaluation.

BACKGROUND

Mechanisms of Retinal Injury from Lasers
and Other Intense Light Sources

Relations between the intensity levels for damage by lasers or other intense light sources have been established independently in several laboratories (59). The criterion for retinal damage was usually a white or edematous spot in the retina large enough to be visible through the ophthalmoscope. On the basis of that work, several different types of damage mechanisms have been proposed, starting with thermal models (27, 28, 55). One of the most comprehensive models is described by Mainster et al. (40). Various forms of thermal models predict which intensity levels will produce injuries in the 1-msec to 1-sec range. Shorter duration exposures appear to require a better understanding of the de-tailed anatomy of the retina, particularly the relation between photo-receptor cells and the pigment granules in the pigment epithelium. To explain this type of interaction, modified thermal models have been pro-posed by Hayes and Wolbarsht (31), Vassiliadis et al. (53), and most recently by Cleary (9) and Barnes (1). The mechanism of injury is

3

modified from a simple thermal model in which the equilibrium tempera-
ture is sufficient to generate steam, deactivate an enzyme system, or
denature some essential cellular component. In the short-pulse domain,
thermal equilibrium is not achieved. As the duration of the pulse ap-
proaches the thermal relaxation time of the melanin granule, it stores
heat and becomes intensely hot (perhaps 300°-400°C). Heat conducted
away from the granule itself is injurious. Also, the highly localized
and uneven heating of the melanin granule could generate photoacoustical
shock waves to produce tissue trauma resulting in a retinal lesion.
With even shorter pulses, in the subnanosecond range, thermal models do
not seem feasible. The rapid energy deposition suggests that the domi-
nant damage mechanisms may be more complex acoustical waves, electron
avalanche, plasma generation, or some other nonlinear process (51).

Pulse durations longer than 1 sec have effects that suggest photo-
chemical or thermally enhanced photochemical models (25, 59). The most
recent data of Ham et al. (29) indicate a dose-related mechanism that is
possibly most effective in the blue (spectrum).

This increased effectiveness of the blue end of the spectrum in pro-
ducing damage is reminiscent of the work of Harwerth and Sperling (30),
in which loss of blue sensitivity was demonstrated by psychophysical
means after exposure of monkeys to high-intensity blue light for extended
periods of time. The action spectra of Ham's long-term retinal lesions,
however, do not agree with the absorption spectrum of the blue cones.
This suggests that the effects seen by Ham may be mediated through some
enzyme or specific biological molecule, possibly in the pigment epithe-
lium rather than in the normal retina. Riboflavin inactivation in the
pigment epithelium has been suggested by Wangemann (58). This region of
transition from functional damage to structural alteration is most impor-
tant. Some kinds of temporary loss of function appear to gradually shift
into permanent damage as the light intensity is increased; both types of
damage depend upon the same mechanism. At other exposure durations and
spectral positions, the damage mechanism may be unrelated to the light
adaptation associated with flashblindness. The temporary function loss
due to flashblindness would result from a different mechanism than that
producing retinal damage lesions, even at threshold intensities.

Functional Disturbances

Two main classes of changes in the visual system result from exposure
to high-intensity photostress. First, greatly lowered visual sensitivity
can be produced temporarily, often termed "flashblindness." Flashblind-
ness may occur even if some protective device is used. As Chisum has
pointed out (8), the few microseconds (or even nanoseconds) that the best
available flashblindness-protection devices take to operate are suffi-
cient to allow large temporary changes in visual sensitivity. In the
second group are the permanent changes, visible lesions in the retina or
decrements in some visual function. All lesions visible in the

4

ophthalmoscope are accompanied by some permanent loss of function in that part of the retina, and possibly in its surrounding areas, although present psychophysical tests may not be sensitive enough to detect easily this change in animals.

Flashblindness: Large Temporary Changes in Visual Sensitivity--Intensive investigation has been carried on in flashblindness, both in anticipating functional loss that might be expected from a given exposure and in design of protection devices. The response times of present-day devices range from a few milliseconds down to several microseconds. Even within this long delay, great difficulty has been encountered in producing a device which can attenuate the light source by more than 1,000. The flashblindness produced within this short time domain shows many nonlinearities. The reciprocity between time and energy, and between area and intensity, does not hold; that is, both Block's and Ricco's laws fail. The site of these deviations from linearity has not been clearly defined. It may be in the photoreceptors, in the intermediate retinal cells, or elsewhere in the nervous system. The spectral distribution of an exposure that produces flashblindness of the lamp is itself important, as chromatic adaptation may change the apparent target contrast and visibility. Most of these aspects, however, are predictable (6, 7, 8).

In dealing with the enormous amount of data on flashblindness and attempting to relate it to retinal mechanisms, we should keep in mind the ideas originally expressed by J. L. Brown (3). In his review he shows that recovery from flashblindness does not involve a single, simple mechanism. Recovery involves those parts of the visual system that usually govern dark adaptation as it is measured conventionally, and it may also reflect neurophysiological effects whose influence is not usually seen in studies of dark adaptation. When the adapting flash energies are sufficiently high, recovery from actual retinal injury may also be involved. Although Brown's empirical equation fits the data for a wide range of conditions, the equation is an empirical one and cannot be expected to cover the extremes.

In this study it is exactly these extreme cases that concern us. Their relationship to most former psychophysical studies of flashblindness is very difficult to assess. Only work in which extremely short flashes and high energy levels were used, such as that by Chisum (8), will be related to the physiological changes attendant upon intensity levels near the injury threshold.

Permanent Change of Function or Visible Damage--Although many attempts have been made to correlate loss of function with exposure to light, the one by Harwerth and Sperling (30) is the most relevant. They found that monkeys exposed for almost an hour every day for a week to fairly high intensity blue light (but not in the flashblindness region) had a permanent decrease in sensitivity to blue light as compared with other parts of the spectrum. Exposures in other spectrum areas produced

5

short-lived or undetectable changes in color vision and general visual sensitivity. This indicates that the blue cone may be especially sensitive to photodegradation. The light used was quite broad band, so it is impossible to tell which specific wavelength was the most effective. Discovering where in the retina the problem lay is also difficult; it could have been the blue cone or the connection to the ganglion cells. It could have been even higher in the visual system. The light source was a large one which affected the whole retina. It is even conceivable that the primary effect was in the pigment epithelium and that this secondarily caused degenerative changes in the blue cones.

Equally important to function loss is the so-called photomaculopathy, the retinal lesion produced by a laser. It has been known from classical times as eclipse blindness, with the sun as the source. Numerous studies have been designed to establish threshold values for the power levels necessary to cause ophthalmoscopically visible lesions (27, 31, 59, 53, 55). These values have been worked out in great detail in relating exposure power levels, duration, spectral distribution, area on the retina, and frequency. Connecting the retinal lesion to functional deficits, however, has been difficult. We do not know, for example, what is the functional loss in the retinal area surrounding the ophthalmoscopically visible lesion. A recovery phase is easily assumed, but its time course is unknown.

Evaluation of Structural Damage and Its Relation to Temporary and Permanent Injury Thresholds--The criterion of injury in most previous studies has been an ophthalmoscopically visible change or lesion in the retina or (infrequently) permanent loss of function. Equally important, however, are the temporary functional changes which occur in parts of the retina that do not appear to be visibly damaged; i.e. each visible lesion may be surrounded by a larger area in which function is not normal, although no evidence of alteration can be seen with the ophthalmoscope. To evaluate temporary changes in portions of the retina exposed to laser levels insufficient to cause visible damage, functional tests have been used: behavioral or psychophysical responses (30, 34, 42, 46, 48) and electrophysiological responses from the retina (2, 32-34, 45, 46, 61) and from the higher visual centers such as the lateral geniculate and cortex (44). Typical of these studies are the psychophysical measurements by Zwick et al. (62) of changes in the measured visual acuity following laser exposure. They found that short- and long-term effects of foveal damage were visual-function changes that involved extrafoveal as well as foveal sites during the first 2 weeks after exposure. A long-term loss of visual acuity occurred that was relatively minor in white light, but was both larger and wavelength specific when color acuity was measured. These losses were restricted to photopic function and could not be demonstrated in the scotopic region. These data correlate well with the experiments by Harwerth and Sperling (30) where blue discrimination was permanently lost after prolonged high-intensity nonlaser stimulation in the blue end of the spectrum.

6

Chisum (8) found that human flashblindness recovery was constant, as a simple function of the integrated luminance of the flash, even though the flashes changed in length. Her work suggested that Block's law (where duration and intensity have a linear reciprocal relation) could not be applied to very short exposures.

All of these psychophysical measurements tend to complicate the interpretation of affected mechanisms within the visual system. Measurements within the lateral geniculate and cortex have been difficult to assess because of the complex aspects of the cell population in these areas (44). Hempel (32) and Priebe and Welch (45) first established the electroretinogram changes after ruby laser exposure. Priebe and Welch carried this further and attempted to correlate electroretinogram changes with changes both in types of retinal lesions seen and in measured retinal temperature. A more direct way to measure these functional changes in the visual system is to monitor directly the retinal cells involved.

The organization of the retina (as now understood in most animals, including man and other primates) is such that when light is received by the photoreceptors (cones and rods), this information is processed in the horizontal and bipolar cells and then integrated by the amacrines and ganglion cells. The ganglion cell is the final summing point in the retina. The optic nerve fibers of the retinal ganglion cells transmit all information back to the lateral geniculate and higher visual centers. However, the primary changes in sensitivity occur in the retina. Initially this happens in the photoreceptors, but the actual site of light adaptation may be at some synaptic connection to bipolars or other retinal cells. To analyze the actual site of change, we need information that can pinpoint the sensitive area and relate it to the damage mechanism. First, the organization of the retina must be understood in sufficient detail to allow characterization of damage resulting from intense light. Then the various changes can be related to specific retinal cells and functions.

Organization of the Mammalian Retina: Types of Ganglion Cells in Cat and Rhesus Monkey

A typical mammalian retina, such as in the cat or rhesus monkey, upon initial examination presents a bewildering array of tiered cells, differing in their connections and their types from one part of the retina to another. Yet underlying all this complexity, some common plan is still discernible. Perhaps these similarities are due to the necessity for convergence upon the relatively sparse ganglion cells, through which all information is transmitted out of the retina.

In spite of numerous arguments on the subject, the present consensus is that the cat does have color vision, albeit possibly limited to that of a dichromat in bright light (12). Tests on the monkey, on the

7

other hand, indicate that it has trichromatic vision similar to that of a normal man (16-20). As the present experimental plan called for developing techniques on the cat to a point where they demonstrate feasibility for use in the rhesus monkey, the functional makeup of the ganglion cells in the cat retina will be examined and compared with that of the monkey retina.

Previous recordings from the cat retina by Granit (26) showed that many recorded ganglion-cell responses carry information that the experimenter, at least, could use to identify the color of the stimulus; i.e., the retinal response provides information to identify the color. Granit's complex theory of dominators and modulators does not furnish a good model for interpreting our present knowledge of retinal function and color vision. His data, however, are hard to dismiss, even though today their interpretation has changed radically. Present investigations on the types of retinal ganglion-cell responses are concerned mostly with connections to intermediate structures in the retina, rather than the distribution of the types of photoreceptors within the receptive field. The functional link between the photoreceptors and the ganglion cells can be studied in two ways. First, the spectral sensitivity of single ganglion cells is analyzed to determine the various cone (and rod) spectral sensitivity curves that may contribute to it. This type of analysis will indicate the spectral sensitivities of all the types of cones. Secondly, the relations of these various classes of cones to each parameter of the various ganglion-cell types must be elucidated. The important parameters are type of influence (excitatory or inhibitory), distribution within the receptive field, and interrelations during light and dark adaptation.

Several experimenters have attempted to record color-dependent responses from cat retinal ganglion cells (35), but the most extensive work is that of Daw and Pearlman (12-15). In their original paper a single type of cone with maximum wavelength at around 555 nm was described. They suggested that this cone, in conjunction with a rod with maximum sensitivity of 500 nm, would enable the cat to discriminate colors in the mesopic range where both rods and cones would operate. Later, however, they found a second cone type, with maximum sensitivity at around 445 nm (43). This, coupled with behavior work of their own and others, suggested that the cat had a color-discriminating system, with two cones and a rod, that was possibly trichromatic in the mesopic range (12). This system was very similar, in principle at least, to some primate systems in which three cone types have been found. Rhesus monkeys and man have them distributed through the spectrum as follows: blue at 445 nm, green at 535 nm, and yellow (red) at 570 nm (15). These are coupled with a rod maximally sensitive at 500 nm. A single ganglion cell may be connected to several types of cones.

The retinal ganglion cells, which become building blocks for the lateral geniculate cells with complicated receptive fields (36), often have complexities of their own. They are often found with one area recovering an excitatory input from one class of cone and with another

8

area, an inhibition from a second class. In man, the rod's activity in the mesopic range does not add precision of color discrimination, rather it adds confusion. This is somewhat contrary to the scheme proposed for mesopic trichromaticity in cats (11). Unequal distribution of photo-receptor classes in the different parts of the ganglion-cell receptive field is well established. Most recent work, however, has concentrated on other aspects of the response; namely, contrast appreciation, discernment of a changing stimulus, or the response latency (22). Based on difference in these parameters, cells have been classified into X, Y, and W types (10, 24, 49, 50). The small-bodied ganglion cells are identified as X and W types (50). They are relatively more numerous than the larger Y cells. The frequency density for X and W cells for a unit area of retina is highest at the area centralis, and falls off sharply with eccentricity. Y cells are relatively more numerous in the periphery, but this seems to represent their uniform distribution coupled with a declining frequency of the other types rather than any great increase in peripheral concentration of the Y cells (50). The classification of X and Y, originally made on the basis of linear (X) and nonlinear (Y) responses (22), is often referred to as sustained and transient (10), with sustained (sluggish) being linear and transient (brisk) being nonlinear.

The X and Y cells often show center/surround organization in the receptive field, with the center and periphery antagonistic to each other. The center of the field often has relatively different characteristics than the periphery. One may respond at the onset of stimulation, and the other at cessation. This in itself has generated the terms "on center" and "off center." W cells have longest latency. The only color responses discussed in detail by most investigators have been identified with the W types (49).

As yet no extensive correlation of the X, Y, and W cells has been established with types of cones, their association with the on and off phases of the responses, or their spatial distribution in the receptive field. Responses have been frequently observed both in the photopic and scotopic phase; i.e., single ganglion cells are connected to both rods and cones (13). Little attempt has been made to differentiate the receptive field into inputs from the various cone types and to relate that differentiation to the X, Y, or W classification.

Our present aim is to stimulate the retina with lasers or other intense light sources and measure the effects of this stimulation upon light and dark adaptation. The initial action of the light (but perhaps not the only action) will be on the rods and cones. It is therefore necessary to determine any differences between cone types, in comparison with rods, in reacting to the intense light stimulus that causes either flashblindness or actual injury of adjacent portions of the retina. Before we can identify changes and quantify their magnitude, the cone types must be well characterized, and the normal organization of the various classes of ganglion cells must be well understood and quickly recognized.

9

A summary of the present classification of ganglion cells in the cat retina is best oriented toward the receptive field. The receptive fields have a concentric organization (49), and the difficulty of finding cells whose responses favor motion detection, implies concentrically shaped fields and linear summations. The central-peripheral organization of the receptive fields is similar to that in the goldfish (47, 56, 57). On/off centers are antagonistic to the off/on peripheral field. Both may be connected to the same or different cone types or even to combinations. Two types of cone inputs to these receptive fields are known--a blue (λ_{max} 445) and a green (λ_{max} 555)(12, 14). One important point to remember is that dark adaptation in the cat has quite a long time course. The cone phase of the dark-adaptation curve recorded from ganglion cells can typically last as long as 20 minutes before the rod phase begins and carries the ganglion cell down to its ultimate sensitivity (44). This is surprising, but all experimenters have seen similar curves. Determining the exact relation between rods and cones in the receptive field is easy because enough time is available to accurately plot the cone phase following even a moderately intense adapting light.

The chief value in examining the rhesus retina is that, from anatomical considerations, at least, it most resembles that of man. Behaviorally also, insofar as it can be checked, the same conclusion can be drawn--that the rhesus eye is a good model for the human eye. Much research has been done on possibly minor differences between the two retinas; e.g., in the distribution of pigment granules in the pigment epithelium and in the thickness of the retina, both of which could influence the relative susceptibility of the rhesus monkey to retinal injury. At the present time, however, the assumption is reasonable that the monkey response to a flashblinding stimulus is quite similar to that of man. Any retinal mechanisms for flashblindness or retinal injury in the monkey should differ quantitatively rather than qualitatively.

In recent investigations of the functional makeup of the monkey retina, DeMonasterio et al.(16, 17, 18) have identified three general classes of ganglion cells. In Class 1 (color opponent), the receptive-field organization has the center antagonistic to the surround on the basis of different cone inputs to each. One cone type is central and on (off); another is peripheral and off (on). These ganglion cells had sustained responses reminiscent (although not specifically identified by DeMonasterio et al. as such) of the X cells, or sustained types, in the cat. More detailed studies are needed, however, to verify this relation. The X and Y cells have not yet been related firmly to any particular cone organization by color or receptive field in the cat, much less any other animal.

Class 2 (transient response) monkey ganglion cells have an intricately structured receptive field; often there are two distinct classes of cones. The receptive field organization usually has the same spectral sensitivity in the center and periphery, but is opposed on (off) to off (on) in response type. Correspondence to the Y-type cell classification

10

in the cat suggests itself, but again discussion is difficult as a correspondingly detailed receptive-field analysis in the cat is missing. Class 3 cells (miscellaneous) in the monkey retina lump together the various types that do not fit either of the other two classes. Cells in Class 3 are less commonly found. Often they do not have a receptive-field organization easily identified as central-peripheral. In general the responses have a short transient (or phasic) on-off character. A few cells in this group are identified as primarily motion detectors. Class 1 is the most common in the fovea, Class 2 is perhaps more common in the periphery, and Class 3 seems to be uniformly distributed over the retina.

The monkey retina organization as given above seems to rule out any major contribution from Class 3 cells, just from the numbers involved. Any study of ganglion-cell function apparently should concentrate on Classes 1 and 2. Class 1 is the most important for form and color perception. Other types might be more important for flicker detection or movement.

Since the ganglion cells are the building blocks for information processing by higher order neurons in the lateral geniculate and visual cortex (19, 20), it is tempting to speculate on the role each class might play in organizing the visual image. Much speculation has produced little progress, however, because of the many choices for additive and subtractive types of interaction in both linear and nonlinear modes. More experiments are needed to limit the speculation to a few clearly defined models. A first step towards understanding flashblindness or permanent loss of function after exposure to lasers or other intense light sources is to catalog the changes in the retinal ganglion cells.

Experimental Approach

Because of the complicated organization and enormous number of retinal ganglion cells, electrophysiological recordings from single ganglion cells can only sample the overall function of the retina. To know just how representative any particular sample is, we must make some approximation of the organization of the retina. Previous studies have given the overall cytoarchitecture. Ganglion cells are connected to intermediate cells such as bipolars and amacrines, and these in turn are connected to each other. The bipolar cells join with the horizontal cells in their connections to the rods and cones (21). As the ganglion cell is the final common pathway for all information leaving the retina, recordings at this point should be able to show any--

(1) distortion of normal function following intense light adaptation;

(2) interruption of function and the time course of any recovery; and

(3) degenerative changes in surrounding areas that may take place at various intervals following the exposure to high intensity light.

11

The experimental plan, simply, is to record from retinal ganglion cells and to classify them in sufficient detail so that salient test points can identify them. Once these characteristic features have been ascertained, then, within a short time after acquiring any cells in an experiment, a highly selected and rapid sequence of tests will classify a cell and allow a prediction of its normal behavior. The next procedure is to apply an intense, chromatic stimulus to adapt either the whole receptive field or a restricted part of it, in order to determine which operating parameters of the cells are changed and how long any change persists. As the central portion of the retina is the most useful in form perception and color vision, our experiments were designed to give data on the area centralis, or fovea. To prepare the way for repeating the experiments on the rhesus monkey, we tested the techniques and the stimulating apparatus on rabbits (which have proven color vision) and cats. Most of these experiments were conducted on adult male and female random-source cats (non-Siamese), because their head structure, with their forward-looking eyes, most closely approximates that of the monkey.

The difficulties attendant upon such a study require that (1) the recording situation be stable enough to allow complete characterization of the cell, and (2) after the intense chromatic light adaptation, the recording conditions remain stable to allow continued recordings of the complete recovery process.

EXPERIMENTAL PROCEDURE

Anesthesia and Surgery

All experiments were carried out under general inhalation anesthesia. Animals were initially anesthetized with ether. When anesthesia was deep enough, an intravenous infusion of gallamine triethiodide (Flaxedil) was initiated. The animal was then intubated and respired artificially with a ventilator (Harvard Apparatus Company, Model 661). Anesthesia was maintained with 70% nitrous oxide/30% oxygen mixture in all animals throughout the experiment. Expired P_{CO_2} was monitored continuously by a Beckman Model LB-1 medical gas analyzer with a NLB-1 pickup. The heart rate was kept within normal limits with the aid of an indicator alarm (Electrodyne MS-25). In addition to the control of gas mixture flow furnished by the anesthesia machine (Ohio Chemical and Surgical Instrument Company, Model 212B), a manometer was installed to avoid any damage to the animal's lung from overpressure during the inspiration and exhalation parts of the respiratory cycle.

The infusion of Flaxedil with dextrose and saline was continued throughout the experiment to assist in fixing the eyes. A local anesthetic (5% lidocaine ointment) was applied to the surface of the conjunctiva before an incision was made to insert the electrode into the eye, and to all other incision margins and pressure points. A heating pad was used to maintain animals at normal body temperature. With these

12

life support systems, the animal remained in satisfactory physiological condition for 24 to 48 hours, and many experiments were of that length.

Although nitrous oxide, even at high pressure, does not produce surgical anesthesia (4, 54), 70% nitrous oxide in oxygen produces a high degree of sedation and analgesia in the cat and is an adequate anesthetic where only mildly noxious stimulants are present; e.g., the direct electrical stimulation of peripheral nerves at frequencies up to 3 Hz or foot-pad shock (54). In our experiments, cats are under deep ether anesthesia during all surgical procedures. In this work the level of ether anesthesia was sufficient to terminate spontaneous respiration and require artificial ventilation. In addition, all cuts were infiltrated with a local anesthetic. Only after surgery was ended was the ether discontinued and 70% nitrous oxide/30% oxygen used. Insertion of the electrode through the pars plana involved no pain and is similar to operations often carried on in humans with only a local anesthetic. The heart rate was continuously monitored, and at no time were changes detected that could be associated with pain perception. The Flaxedil drip was not required to relax the animal, but helped achieve the high degree of eye immobility required for single-cell retinal recordings (22). It has been established that Flaxedil has no effect on cat retinal ganglion-cell responses (23). Because of these considerations, nitrous oxide and Flaxedil have been routinely used by all workers in this field.

Nitrous oxide is used by us and others because it has only slight effects on evoked CNS responses as compared to the strong central depression produced by other volatile anesthetics and barbiturates (54). A depressive action in the retina has also been seen with some of these anesthetics (52). Minimizing drug effects on the CNS is obviously important when studying the activity of the visual system.

Optical Stimulus

The optical stimulator was adapted from a system described previously by Wagner et al. (56). A diagram of the present system is shown in Figure 1. The source light was a GE projection light (type CPG) featuring a concentrated coiled filament. The filament current was stabilized by a regulated DC power supply at 17 A, the filament with a color temperature of approximately 2850°K. The lamp output was monitored by a photodiode and was maintained constant by filament-current adjustment.

The optical stimulator had two pathways, essentially equivalent optically, which could be varied independently. Each pathway had a collimated region between lenses L_1 and L_2 to allow placement of interference filters. These filters--two-cavity visible-pass filters (Dietrich Optics) with approximately a 3- to 5-nm halfwidth--had λ_{max} at each 10 nm from 420 to 660 nm. All filters were individually calibrated. Table 1 shows the characteristics of the interference filters used with their pass bands.
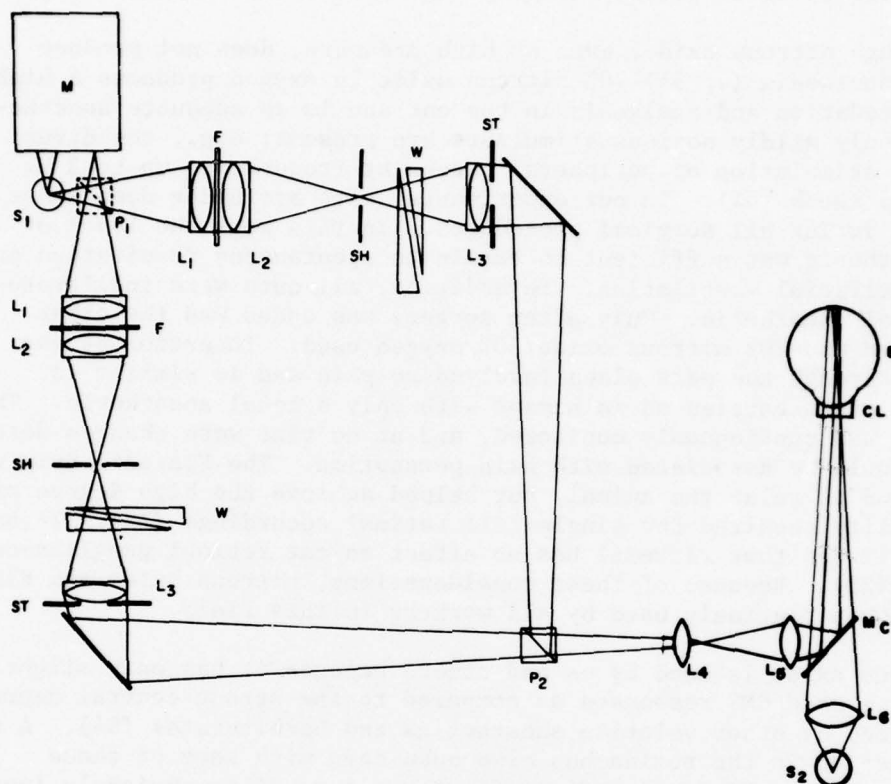
13

Figure 1. Schematic diagram of the optical stimulator and its relation
to the animal's eye. F--filter; L_1, L_2--collimating lenses; L_3--
field lens; L_4, L_5, L_6--projection lenses; M--monochromator; P_1--
separating cube; P_2--combining cube; SH--shutter; ST--field lens
aperture stop; W--neutral-density wedge and compensator; E--eye;
CL--flat-faced contact lens; S_1--source lamp; S_2--background lamp;
M_C--combining pellicle mirror. The beam between L_1 and L_2 is
collimated, allowing the use of interference filters.

Each shutter consisted of an electromagnetically driven vane in an
aperture after a design given to us by H. K. Hartline (personal communi-
cation, Rockefeller University). The neutral-density circular wedge (W)
was a Kodak Wratten type-M, deposited-carbon, with a 3.0-log range. An
aperture stop (ST) was mounted over the field lens (L_3) and could be
varied in size and position. This aperture stop was attached to the
carriage of an x-y plotter, Varian Model 1016. This carriage was con-
trolled externally and was electrically linked to a slave x-y plotter
to indicate the position of the aperture within the stimulus field at

14

TABLE 1.   WAVELENGTH CHARACTERISTICS OF FILTERS USED

Wavelength	Half bandwidth	Percent transmission
420	6.6	47
440	4.6	54
460	5.0	55
480	2.9	51
500	3.5	53
520	4.2	59
540	3.7	59
560	4.0	57
580	4.3	56
600	4.5	52
620	5.5	58
640	4.9	57
660	5.7	49

any given time. The aperture position could be moved either manually through the x-y plotter with variable-voltage dividers or by function generators causing the voltage to oscillate about any predetermined position in any axis.

The beams from the two channels were brought together in the combining cube (P_2), then passed through a series of lenses and a final mirror (MC). The final lens (L_5), in combination with a flat-faced contact lens to eliminate the cornea as an optical element, imaged the filament in the plane of the iris in a Maxwellian view to allow the field aperture (ST) to be focused on the retina. The beam was approximately normal to the retina to eliminate any changes in stimulus-response relations due to the Stiles-Crawford effect. The last mirror (MC) was partially reflecting to allow a background light from a third channel to flood the whole retina. The background light was a GE M-17 projection lamp (Code EJA) and had a spectrum similar to the source lamp (S_1) when operated at 80% of its rated (21 V) voltage. The major pass bands of the broad-band Wratten filters used to modify the spectrum of the third channel are shown in Table 2. The positions of the stimulating light and the recording electrode were viewed through a biomicroscope focused on the retina. In one channel, a Bausch and Lomb monochromator (Model 33 86 45 38) was arranged (as shown in Fig. 1) so that a continuously variable selection of wavelengths could be used for the stimulus. The monochromator was modified to place the exit slit beside the entrance slit as required by the design of the optical system. The optical stimulator was also designed to allow using a high-intensity adapting light, such as a laser or xenon arc, to replace the monochromator.

TABLE 2. WRATTEN FILTER CHARACTERISTICS

Wratten filter No.	Major pass band
15	510 - 680
21	540 - 680
22	540 - 680
30	410 - 480
	560 - 680
31	415 - 480
	580 - 680
47A	410 - 540
47B	410 - 500

The optical system output was calibrated with an Epply thermopile (type 12, junction linear, with a quartz window). The sensitivity of this thermopile, in turn, was calibrated against a secondary standard lamp (Epply type NALCO A-10), whose initial calibration is traceable to the National Bureau of Standards.

The procedure for calibrating the thermopile against the standard lamp and standardizing the optical-stimulator output are described by Wagner et al. (56). The calibrated thermopile was placed at the filament image formed by the final lenses (L_5 and L_6). In this position, measurements were taken of intensity with the various filters and neutral-density wedge settings, at the various source and background lamp currents, and at selected wavelengths from the monochromator. Other measurements were taken at the image plane formed by lens L_5 for the aperture (ST). From those measurements a scaling factor could be determined to allow all measurements made on the filament image to be transposed into the aperture image plane. For most filter combinations, the sensitivity of the thermopile was not sufficient to make all measurements directly in the aperture image plane.

The demagnification of the optical system--that is, the ratio between the sizes of the field aperture (ST) and the size of the focused image on the retina--was found experimentally. An iris diaphragm was used as the field aperture and was adjusted so that its projected image on the cat retina was exactly the size of the optic disc to be measured with a microscope. Although this ratio was not checked for every eye, we expect only minor variations in this ratio to exist from one cat to the next. In our experiments the major refracting element, the cornea, is eliminated as an optical surface. The only biological variable from one cat to the next would be the power of the lens. As the accommodative mechanism is paralyzed, no changes can take place during the course of experiments, and the lens-size variation from cat to cat is probably very negligible in relation to the size of the retinal images that are used.

16

Electrophysiological Recording Equipment

The electrodes used were similar to those described by Levick (37, 38) and were made of tungsten wire electrolytically sharpened to be less than 0.5 μm in diameter. The tip was pushed into a finely drawn glass capillary until it protruded 2 to 5 μm. The capillary wall was less than 0.1 μm at the junction of the tungsten and the capillary. The other end of the glass capillary was then glued to the shank of the tungsten wire with quick-set epoxy cement (Devon 5-minute) under direct visual observation. The electrode tip was then coated with platinum black and inserted into a trochar carrier. Details of the electrode and carrier are shown in Figure 2. The trochar was pushed through the sclera in the region of the limbus and positioned within the eye. The electrode could then be extended through the trochar bushing, and the electrode tip, without being damaged, placed in contact with the retina. The signal from the electrode was led into the input probe (Fig. 3) designed to be used with a balanced amplifier (Fig. 4) similar to that described by MacNichol and Bickard (38).
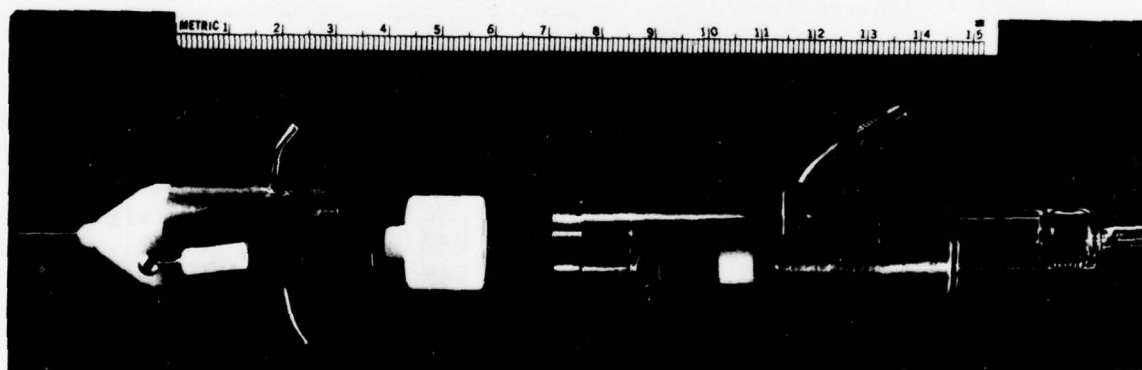

Figure 2. Electrode and carrier. The electrode is hydraulically driven with the plunger of the hypodermic syringe mounted on the right-hand side. The remote control of the hydraulic drive is connected at the end of the syringe. A portion of the plunger is shown towards the left. The electrode is attached to the Teflon cylinder in the center, which in turn is moved in and out by the plunger of the hypodermic syringe. On the left is the trochard within which the electrode moves. The central connection on the left is the ground connection; the upper connection on the right is a coaxial connector with the core connected to the recording electrode; the two arms at the top and bottom on the left-hand side are attachments for springs to hold the system in place. When in use the trochar is mounted snug against the limbus of the eye.
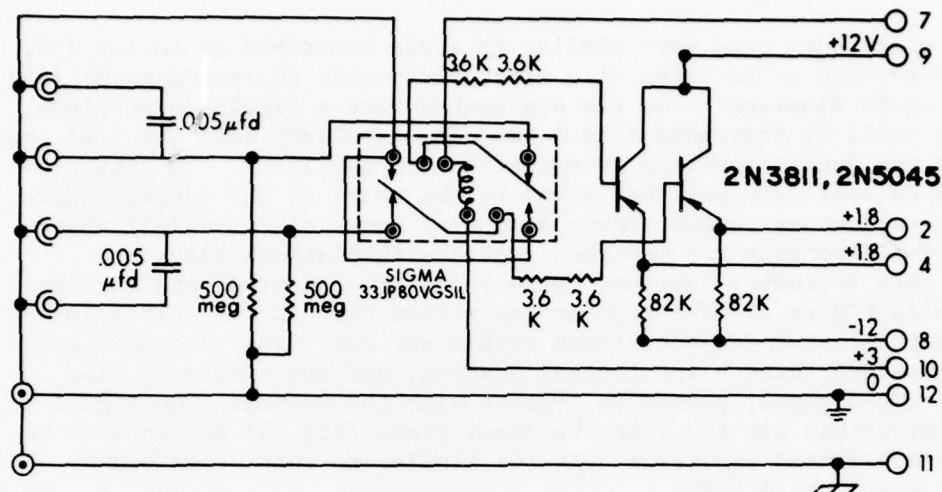
17

Figure 3. Input probe for physiological amplifier. The relay is a special high-resistance type so that the input impedance is not lowered. The amplifier (Fig. 4) has a balanced input, but one side is generally grounded.

This combination is quite stable, nonmicrophonic, and combines the high- and low-pass filters necessary to get rid of extraneous noise and improve the signal-to-noise ratio for nerve impulses. The output signals of this amplifier are put through a delay line noise filter (5). This delay line filter can be tuned to the shape of the impulse, increasing the signal-to-noise ratio by rejecting all noise not having a waveform similar to that of the impulse, generally of very low amplitude. The output of this filter is a sharply defined pulse with an amplitude proportional to the integrated energy of the original impulse. This allows use of a window discriminator. The advantage of this filter system is that the electrode is not required to completely isolate each ganglion cell. A single electrode may record from two or more units simultaneously, with the impulses easily distinguished from each other by this filter and window-discriminator combination.

Most ganglion cells used in this study could be sufficiently isolated by electrode placement and did not require using the delay line filter. When two ganglion cells were seen simultaneously, however, usually one could be selected in preference to the other by various settings of the filter and window discriminator. Although only one cell was usually studied at a time, the possibility remains with this technique for several to be studied simultaneously. The criterion for deciding if the recording was from one or more units was based on a comparison between the sizes and shapes of successive nerve impulses. The
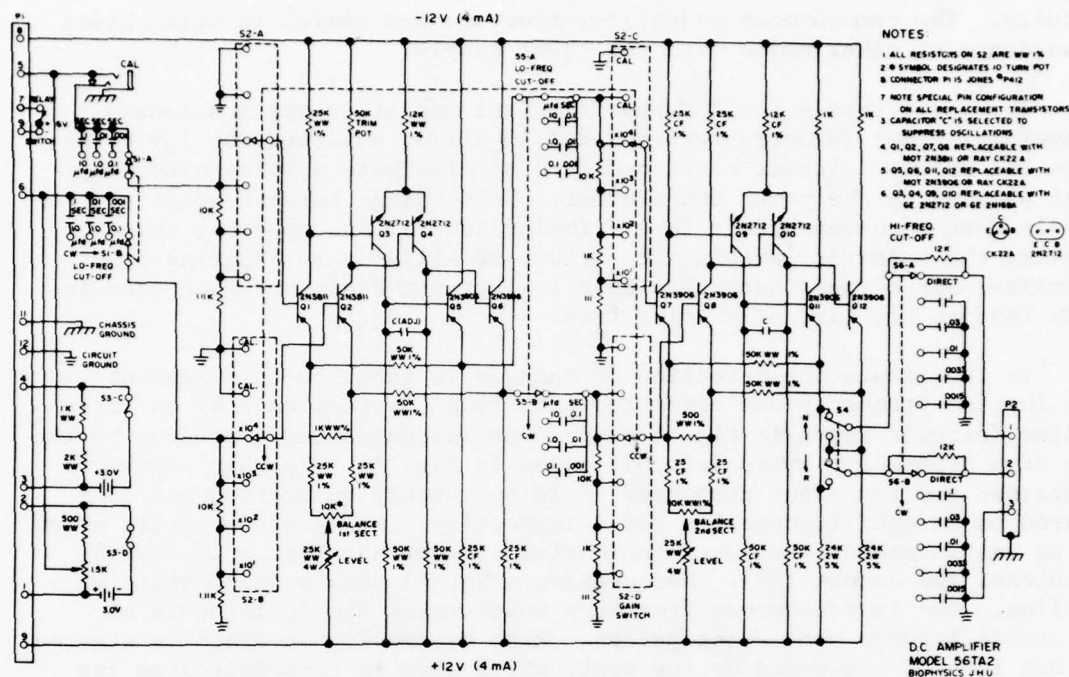
18

Figure 4. Physiological amplifier. This amplifier has been modified
from the original circuit given by MacNichol and Bickard (38). It
has an overall gain of 20,000 with a balanced output with the input
probe shown in Fig. 3. In this configuration with a solid-state
power supply, drift is less than 100 µV per hour and no balancing is
required from day to day. The filters allow rejection of most noise
within the frequency range of the nerve impulses.

occasional presence of very large impulses in the response was almost
always the algebraic summation of two impulses, a certain indication of
multiple units. Changes in instantaneous frequency between successive
spikes generally suggested that multiple units were present. These cases
were analogous to two oscillators running at slightly different frequen-
cies.

Although the amplifier used (Figs. 3 and 4) was a balanced-input
double-sided amplifier, this feature was not needed in our recording
situation to reduce 60-cycle interference. The input signal contained
only a small component of 60-cycle pickup. This low level was achieved
by carefully placing major pieces of electronic equipment, using low-
resistance metal microelectrodes, and laying out the system so as to

19

eliminate ground loops. Elaborate shielding of the animal was not required, although all strong-interference generators were shielded locally. The common-mode rejection, however, was useful in eliminating transients or other noise from the power supply.

The power supply for the physiological amplifier was a standard commercial model (Electrostatics Model 10-1212), selected for low noise, with the printed circuit board modified to eliminate a voltage-sensing lead passing by the power transformer. This change cut the noise and ripple down to unmeasurable levels (below 50 μV). No need was found to convert the batteries within the circuit to solid-state floating power supplies, since these batteries have low current drain and when used in this fashion are virtually noise free.

To facilitate the detection of changes in ganglion-cell response, the impulse frequency was converted both to an average rate by an integrator (circuit shown in Fig. 5) and to an instantaneous frequency by the use of a hyperbolic sweep (circuit shown in Fig. 6). In this way both sustained and transient responses could be quickly quantified and displayed on an oscilloscope for rapid inspection. Using a hyperbolic sweep as an instantaneous frequency-indicating circuit has been suggested by MacNichol and Jacobs (39). Our version (Fig. 6) uses a solid-state multiplier. The instantaneous frequency meter takes the reciprocals of intervals between succeeding pulses. Each hyperbolic waveform is started by one impulse and ended by the next, which also in turn initiates its own hyperbolic sweep. The end of each hyperbolic sweep is indicated on the oscilloscope display by a bright spot. A typical display is shown in Figure 7. This type of display allows rapid evaluation of any changes in the response frequency as a result of changes in either the stimulus or the adaptation level.

The coordinate in all figures showing ganglion-cell responses is log sensitivity, and the intensity calibration is given for the zero log value in absolute units. This value refers to the stimulus on the retina in microwatts per square centimeter. No correction was made for variations in the ocular-media transmission as a function of wavelength. The size of the stimulus on the retina was calculated from the system demagnification after this was experimentally determined as described on page 16 This value is, however, corrected for all wavelengths and for any filter or combination of filters used in the optical stimulator. A 1-log-unit increase in sensitivity means the ganglion cell is 10 times more sensitive, or in another way, one-tenth the energy is required to stimulate as in the zero log situations.

Experimental Design

The anatomical structure of the cat eye and its resemblance to the monkey eye, along with the possible similarity in function between the monkey and cat retina, allowed us to formulate the present program. The
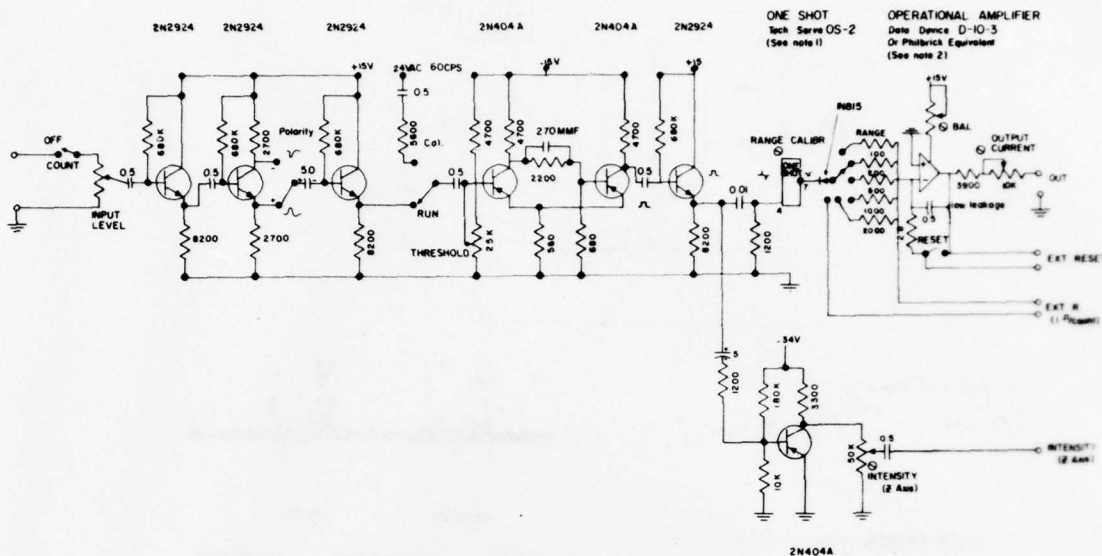
Figure 5. Frequency-to-analog conversion circuit. A given pulse can be selected and the frequency quantified by integration. The "One Shot" is a commercially available Schmitt trigger, accepting a wide range of positive pulses and giving a precisely controlled, uniformly sized pulse output which the operational amplifier integrates. The output voltage level is then a function of the pulse frequency. The intensity modulation shows which pulses in the mixed-size train are counted so that threshold can be properly set. (Circuit courtesy of J. Schainbaum and F. Hanson, University of Pennsylvania, personal communication.)

overall objective is to examine the type of receptive field and determine as rapidly as possible its classification and pre-light-adaptation values for each cone-system input to each part of the receptive field. An adapting stimulus is then given, and any changes are documented. To provide basic working tools, we compiled a dictionary of the common cell types and developed techniques to determine quickly the category appropriate for each cell. Not only must the response characteristics be given, but the types of photoreceptors that are connected to the ganglion cells must be known; e.g., whether one or more classes of cones are connected, how each is distributed within the receptive field, and when each is excitatory or inhibitory. If the rod system is connected, then its interaction with the cone types must be predictable.
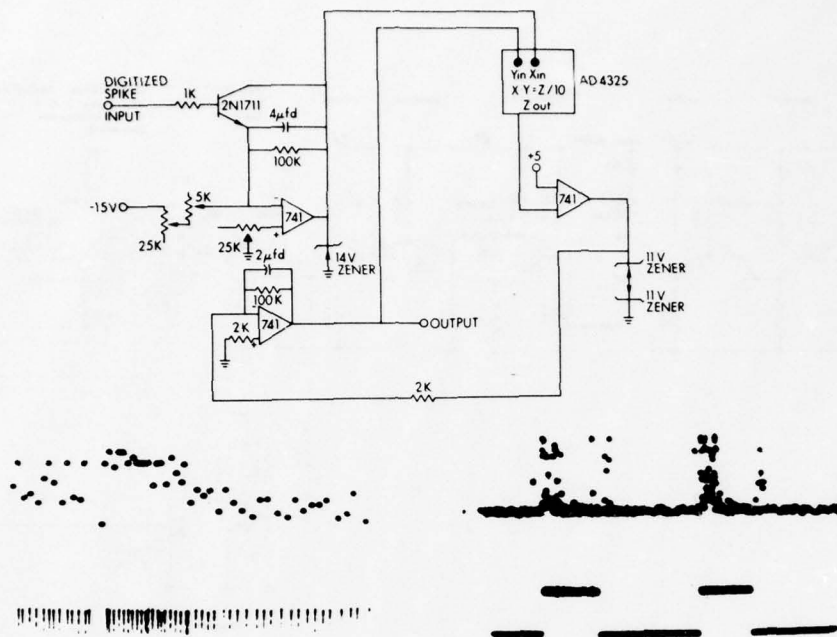
21

Figure 6. Hyperbolic sweep for instantaneous frequency display. In the
lower left corner is a display of the operation: individual nerve
impulses are shown at the bottom; and above, the height of the dots
is directly proportional to the interval between the impulses. In
the lower right is shown a typical response of a cell to pulses of
light indicated by the upward deflection of the lower trace. Each
light pulse is 0.75 sec. The cell has both an on and off response,
with the off response more vigorous for the selected stimulus con-
ditions. Both left and right displays are 5 sec long.

Of no less importance is the part each photoreceptor plays in dark
adaptation and the contribution of each to the information carried by
the ganglion cell at photopic, mesopic, and scotopic ranges. Spectral
sensitivity and changes in receptive-field makeup must be known also.

Most data points were based on a constant-response technique; i.e.,
when a parameter changed, the stimulus intensity was varied sufficiently
to obtain a response equal to the original (or criterion) one. Some
data points were obtained by silent substitution. In this technique the
stimulus is presented immediately after the control stimulus for an on
response (or immediately preceding the control stimulus for an off
response). If the two stimuli are equivalent, switching from one to the
other evokes no response. Some care is required, however, to distinguish
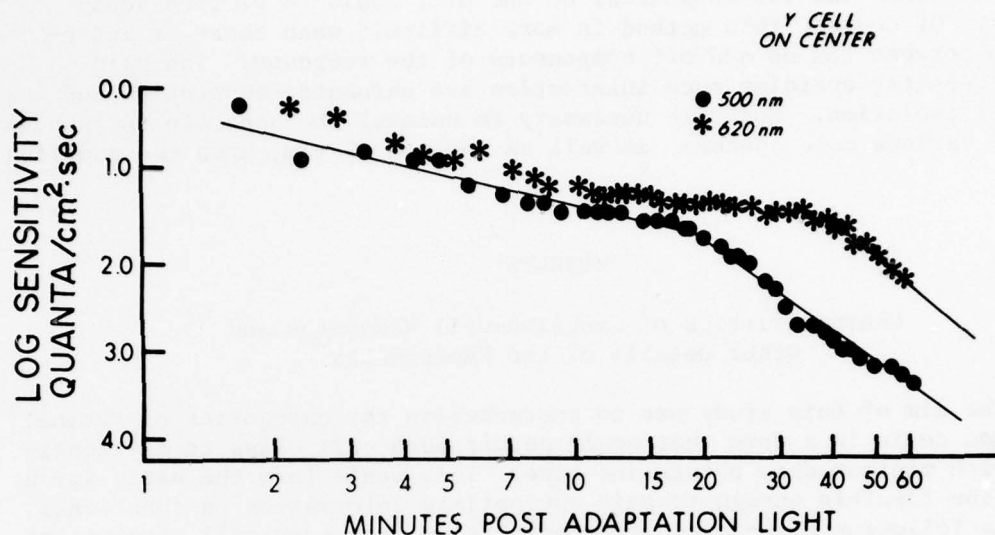
22

Figure 7. Dark adaptation of central response in a Y cell. This cell is located near the optical axis of the eye, in the area centralis. The test stimulus is a 200-μm-diameter spot in the receptive-field center. This is an on-center/off-periphery cell. The dark adaptation curve for a 500-nm test stimulus showed a slow cone adaptation with a very sharp rod onset at about 18 min. With a 620-nm test stimulus, the rod-cone break took approximately 35 min. The cone system shows little adaptation and a correspondingly small recovery. The 555-nm cone system is more sensitive to the 620-nm filter than is the 500-nm rod system, thus the rod-cone shift is delayed relative to that obtained with a 500-nm test stimulus to which the rod system is more sensitive. Zero log units on the sensitivity scale equals 3.5×10^{12} quanta/cm^2·sec on the retina for both filters (15.1 μW/cm^2 at 500 nm, 3.3 μW/cm^2 at 620 nm). The adapting light used a Wratten filter #21 for 3 min at 4.3×10^{14} quanta/cm^2·sec (134 μW/cm^2), followed by a 6-min exposure using Wratten filter #30 at 4.3×10^{14} quanta/cm^2·sec (127 μW/cm^2).

between on and off responses when both cannot be balanced simultaneously. In general this silent-substitution technique can be used to get very precise measurements, but only when the proper value of the stimulus is already known, with a fair degree of accuracy, from other techniques. Neither the constant-response nor silent-substitution technique can be used when the character of the response changes from on to off as the stimulus is changed. However, the on portion of the response could be made the same as the control response, while the off portion was ignored;

23

then the off portion made the same as the control, while the on was ignored. Thus the two responses, on and off, could be plotted separately. Of course, this method is more difficult when there is interaction between the on and off components of the response. The main techniques for avoiding such interaction are chromatic adaptation and spatial isolation. Both are necessary to unravel the separate influences of the various cone systems, as well as the rod system, upon the ganglion cell.

RESULTS

Characteristics of Ganglion-Cell Responses and Other Details of the Experiments

The aim of this study was to characterize the categories of retinal ganglion cells in a form that would permit each cell class to be identified with minimum data points and time. This would form the basis for a technique flexible enough to gain appropriate information on functional changes following high-level light adaptation from each cell appropriate to the organization of that class. In developing the technique, we compared various kinds of electrodes, including glass-coated platinum-iridium and epoxy-insulated tungsten. These two electrode situations were evaluated in the rabbit eye by varying the exposed tip length and insulation thickness. The ease of fabrication and high number of successful recordings in every way favored the Levick-style tungsten electrode described on page 17. Our results are of work using this electrode. A stable headholder, constructed to allow adequate monitoring of all vital physiological signs, allowed our experiments to last 2 or more days. Such long experiments were helpful in screening as many types of cells as possible. When an animal is to be used more than once, however, such long experiments are not feasible because recovery is often unsuccessful. We found it necessary to relax all tension on the eye occasionally during the long test runs. The preliminary experiments were terminal ones so that maximum data could be collected. Sufficient experience has now been gained, however, to indicate that repeated recordings can be made from a single animal if proper sterile precautions are taken, and if the eye and contact lens are stabilized by suturing under the muscles rather than suturing the conjunctiva directly to a Flieringa ring as in the present series.

The ganglion-cell responses of the cat have a very short latency as compared with those of the frog or goldfish; several rapid-acting electrode aids were needed to help with signal discrimination. Most experiments were designed to use a constant-response criterion. In a given experiment it was not necessary to count impulse frequencies, only to determine if the response frequency was the same as the criterion or in which direction it had changed. This simplified data acquisition made it possible not only to measure several parameters such as wavelength sensitivity, sensitivity of response as a function of position within the

24

receptive field, and changes in rate or level of dark or light adaptation, but also to plot the values in real time during the experiment. This type of data procession increased our ability to detect any variations in receptive-field contributions from each cone- or rod-system input resulting from adapting lights in either the center, surround, or full field and from various spectral compositions and intensities.

During a single recording session we could experiment upon many ganglion cells in one eye. Individual cells have been held for 10 hours or longer. Recording times of at least 4 hours were necessary to plot full-dark-adaptation sensitivity curves showing the rod-cone shift. In the cat a single dark adaptation may take as long as an hour, as shown in Figure 7. In this type of experiment it is necessary to go through the dark-adaptation process at least twice, possibly more often, if this parameter varies as a result of intense chromatic light adaptation. In the cat the dark-adaptation course may last as long as an hour to show the rod-cone break clearly.

Categories of Ganglion Cells and Chromatic Adaptation

All ganglion cells were tested to place them in the X, Y, and W classification and to characterize the input from cone and rod systems, the type of color coding if any, and the spectral properties of the various parts of the receptive field. Most cells studied were X or Y. W cells were encountered rarely and were not especially sought. The sluggish response from W cells made data acquisition from them take an excessively long time. We were unable to get a complete series from any W cell of the spectral distribution within the receptive field, nor could we get reliable dark-adaptation curves. Many cells did not fit into the X, Y, or W classification scheme.

Some typical X-cell responses are shown in Figures 8-15. Both X and Y cells usually had the center-surround organization. A typical receptive-field plot, in this case of a Y cell, is shown in Figure 16. In some cells the relative sensitivity of the on and off responses was approximately constant in all parts of the receptive field, indicating that all cone systems overlapped each other concentrically, with the same relative distribution over the field. Both on-center and off-center types were seen in which the center and the surround had two spectral sensitivities. This is shown in Figures 17 and 18 for a Y cell. The underlying organization of the cat receptive fields, with the central responses opposed to the peripheral ones, appeared to be much the same as in the goldfish or the monkey, although not as clearly related to color vision. The shapes of the response curves of the separate cone systems are found in Figures 8, 9, and 11. Both (or either) the center and the surround could be on or off, and either could have several cone systems in it.
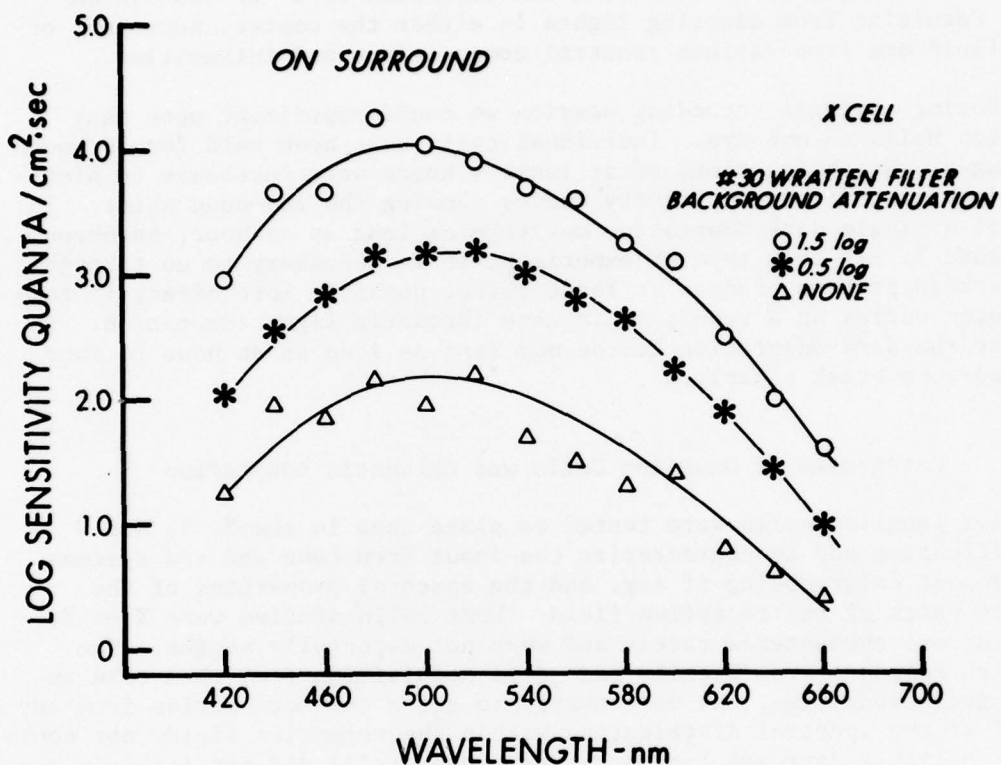
25

ON SURROUND

X CELL

#30 WRATTEN FILTER
BACKGROUND ATTENUATION

○ 1.5 log
✳ 0.5 log
△ NONE

LOG SENSITIVITY QUANTA/cm²·sec

WAVELENGTH - nm

420   460   500   540   580   620   660   700

5.0
4.0
3.0
2.0
1.0
0

Figure 8. A spectral sensitivity of surround process of an off-center/
on-surround X cell. This on response shows no change in shape with
background adaptation by a #30 Wratten filter. The curve matches
the Dartnall nomogram with a λ_{max} of 500, and the light levels indi-
cate that it is probably a cone system rather than a rod system.
This lack of fractionation of the response indicates that this is
probably a contribution from a single cone type. Zero log units on
the sensitivity scale equals 3.5×10^{14} quanta/cm²·sec (15.1 µW/cm²
at 500 nm) on the retina, and zero log units on the background
equals 4.1×10^{13} quanta/cm²·sec (127 µW/cm²). The stimulus is an
annulus of 1.25-mm inner diameter, 3.0-mm outer diameter, on the
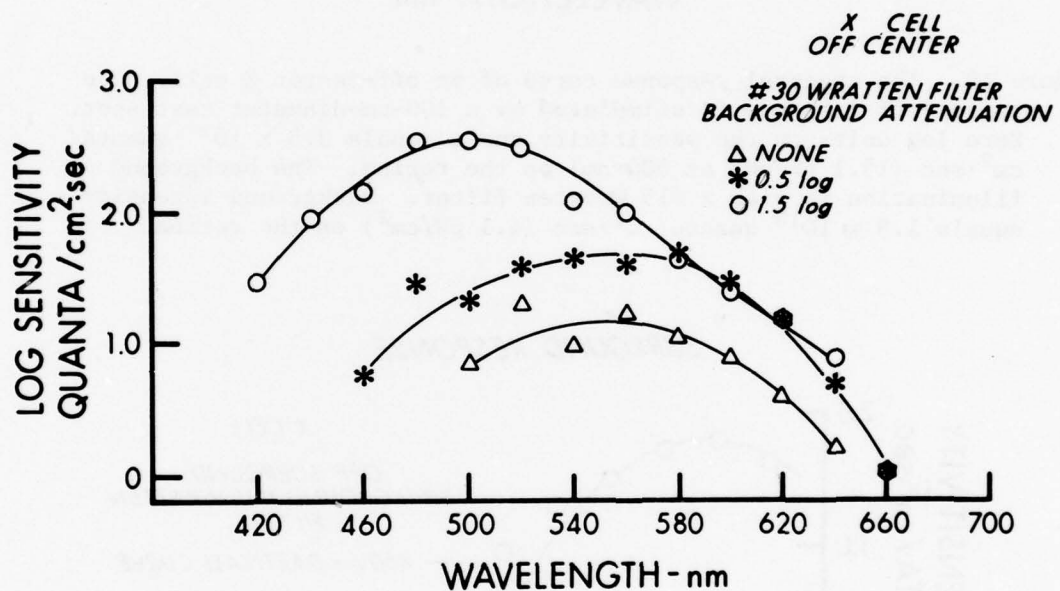retina.

Figure 9. Central responses of an X cell as modified by background
chromatic adaptation. Zero log sensitivity plot equals 3.5×10^{14}
quanta/cm^2·sec (15.1 µW/cm^2 at 500 nm) on the retina, and zero log
units on the background equals 4.1×10^{13} quanta/cm^2·sec (126 µW/cm^2).
The size of the test spot is 200 µm for zero and 0.5-log attenuation
and 100 µm for the 1.5-log attenuation. Two cone systems appear to
be represented in the center, a 555 and a 500 nm. The background
differentially suppressed the 500-nm system, as shown in the lower
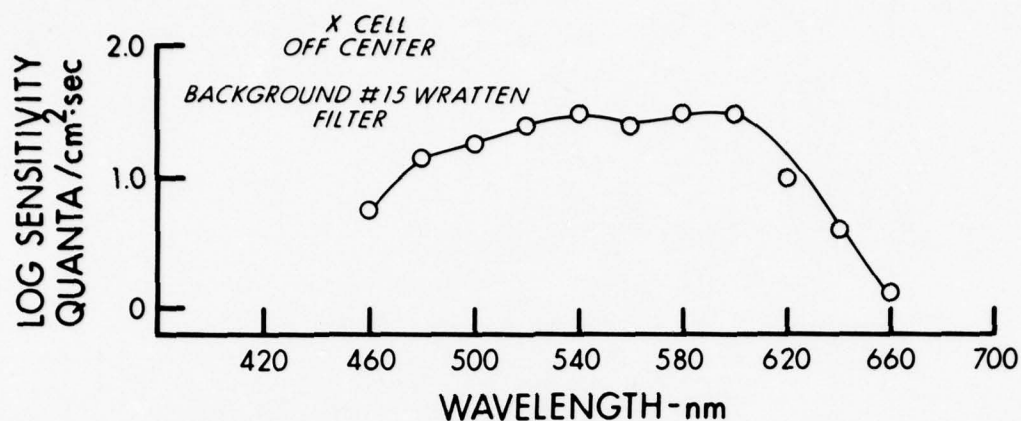curve which seems to be only the 555-nm cone system.

Figure 10.   The spectral response curve of an off-center X cell.   The
center-off response is stimulated by a 100-μm-diameter test spot.
Zero log units on the sensitivity scale equals 3.5×10^{14} quanta/
$cm^2 \cdot sec$ (15.1 μW/cm^2 at 500 nm) on the retina.   The background
illumination is with a #15 Wratten filter.   Background intensity
equals 1.3×10^{13} quanta/$cm^2 \cdot sec$ (4.1 μW/cm^2) on the retina.
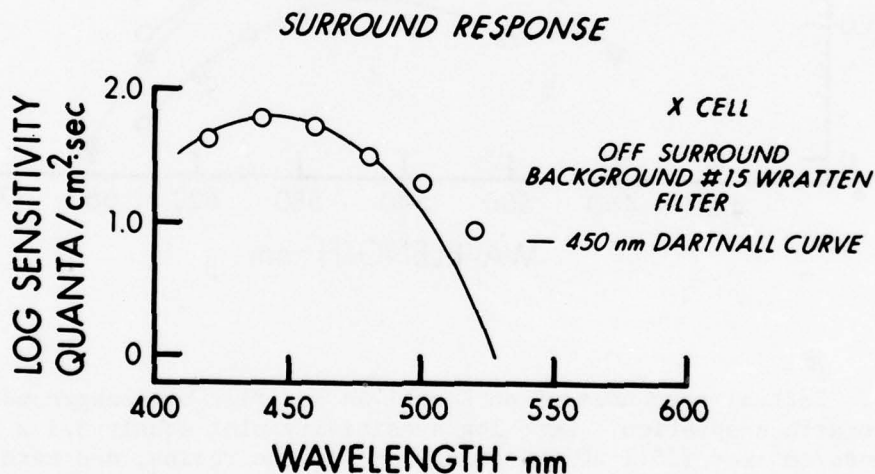

Figure 11.   Surround response of an X cell.   This is an off response
tested with an annulus of 1.1-mm inner diameter, 3.0-mm outer diam-
eter, on the retina.   A strong green background shows the response
of a blue cone curve peaking at about 450 nm.   The comparison with
Dartnall's nomogram curve for 450 nm indicates that the response
curve is slightly broader than the nomogram.   The sensitivity scale
is corrected to show equal quantum flux at all wavelengths.   Zero
log units on the sensitivity scale equals 9.0×10^{13} quanta/$cm^2 \cdot sec$
on the retina; this is 3.8 μW/cm^2 at 500 nm.   The background equals
6.3×10^{14} quanta/$cm^2 \cdot sec$ (2.0 μW/cm^2) on the retina.
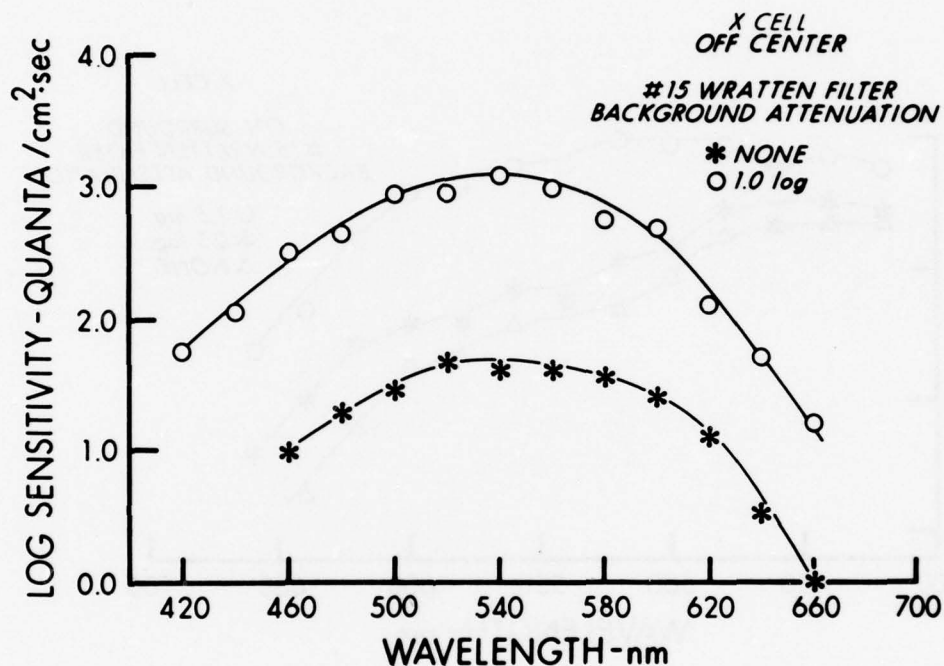
28

Figure 12. A central off response of an X cell. The cell is located very near the area centralis and has possible contribution from a 500- and 555-nm cone. A strong blue background depressed the short-wavelength end of the curve relative to the long-wavelength end. The sensitivity scale is corrected to show equal quantum flux at all wavelengths. The test stimulus is 200 μm on the retina. Zero log units on the sensitivity scale equals 5.67×10^{14} quanta/cm^2·sec on the retina; this is 23.93 μW/cm^2 at 500 nm. The background equals 2.0×10^{13} quanta/cm^2·sec (6.5 μW/cm^2) on the retina.
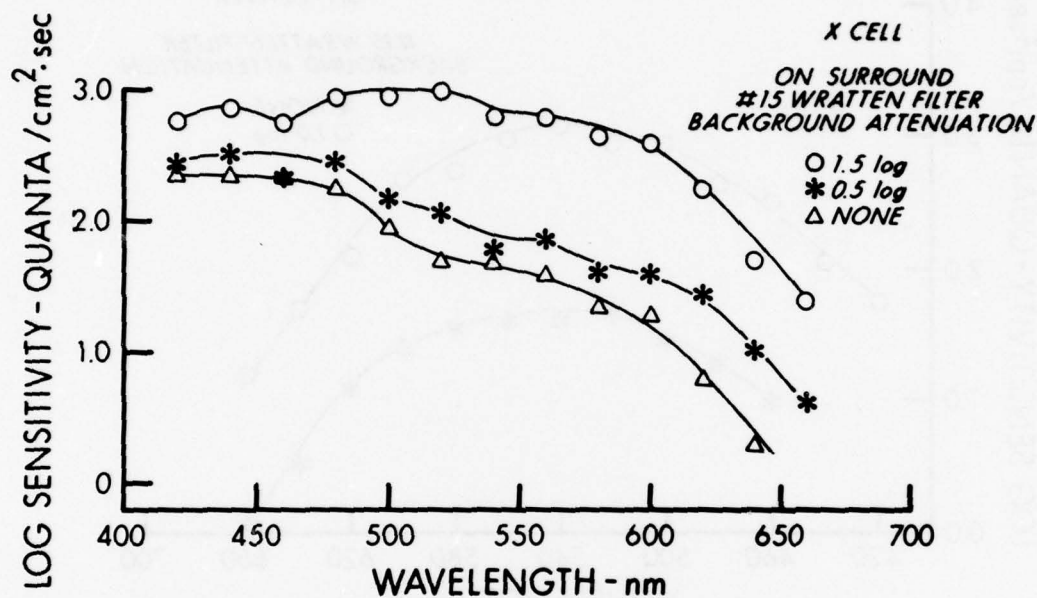
Figure 13. Spectral sensitivity of the surround of an X cell. The test
stimulus is an annulus of 1.1-mm inner diameter, 3.0-mm outer diam-
eter, on the retina. A green adapting background attenuates the
center of the curve with relatively less effect on the ends. This
is especially notable when the top and bottom curves are compared.
The sensitivity scale is corrected to show equal quantum flux at all
wavelengths. Zero log units on the sensitivity scale equals 3.5×10^{14} quanta/$cm^2 \cdot$sec on the retina; this is 15.1 μW/cm^2 at 500 nm.
The background at zero log units equals 6.6×10^{13} quanta/$cm^2 \cdot$sec
(21.6 μW/cm^2) on the retina. This cell may have contributions from
all three cone systems.
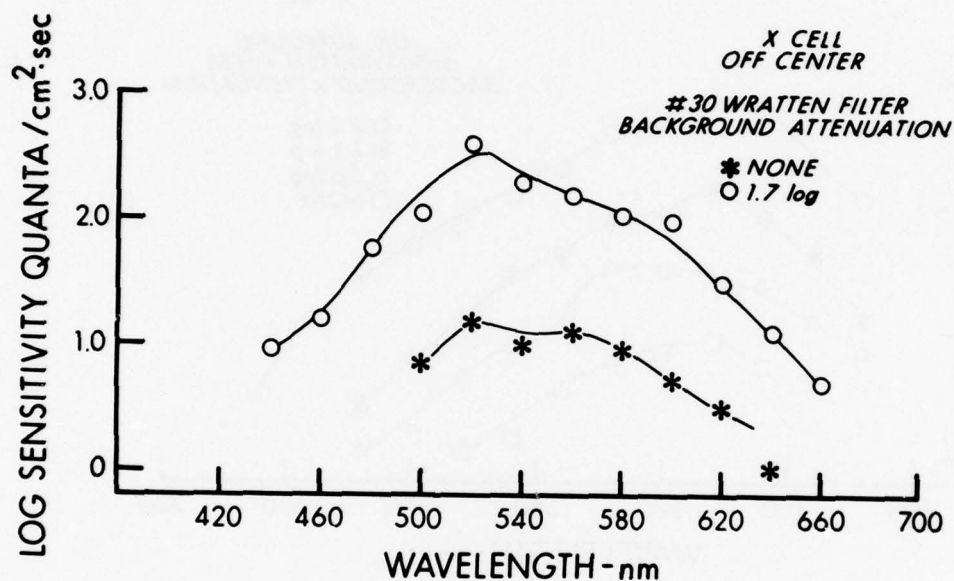
Figure 14. Spectral sensitivity of the center response of an X cell. A 200-µm test stimulus was used. The sensitivity scale is corrected to show equal quantum flux at all wavelengths. Zero log units on the sensitivity scale equals 3.5×10^{14} quanta/cm$^2 \cdot$sec on the retina; this is 15.1 µW/cm^2 at 500 nm. The background at zero log units equals 7.5×10^{13} quanta/cm$^2 \cdot$sec (20 µW/cm^2) on the retina. Other characteristics of this cell are shown in Figs. 15 and 22.

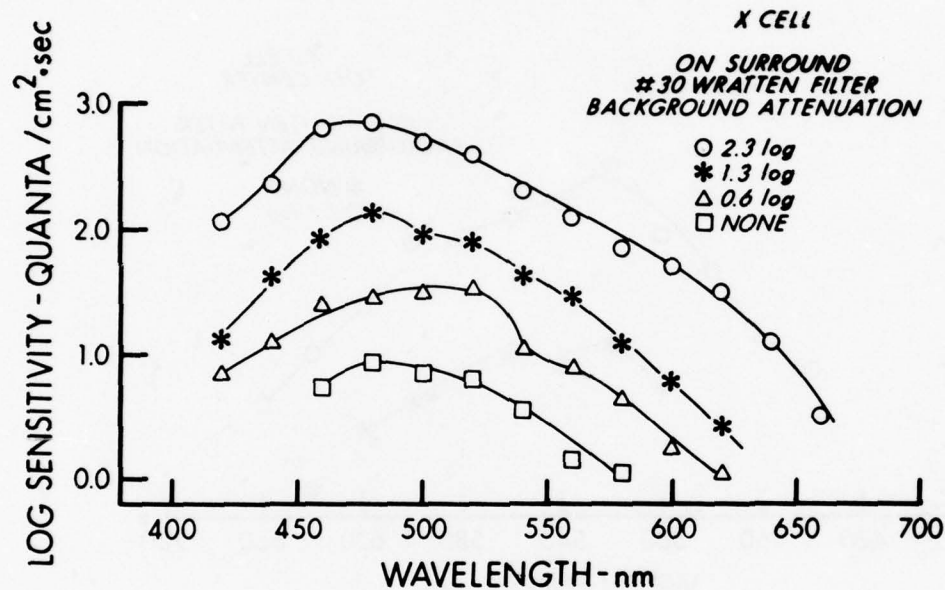Figure 15. A spectral sensitivity profile of the surround response of an X cell. This is an off-center/on-surround cell. The stimulus was an annulus of 1.35-mm inner diameter, 3.0-mm outer diameter, on the retina. Suppression of the 450-nm cone system is shown with a #30 filter. Possibly both a 450- and a 500-nm cone contributed to the response. The sensitivity scale is corrected to show equal quantum flux at all wavelengths. Zero log units on the sensitivity scale equals 1.39×10^{14} quanta/cm$^2 \cdot$sec on the retina; this is 6.0 μW/cm^2 at 500 nm. For the background, zero log units equals 2.6×10^{14} quanta/cm$^2 \cdot$sec (80 μW/cm^2) on the retina. Other characteristics of this cell are shown in Figs. 14 and 22.
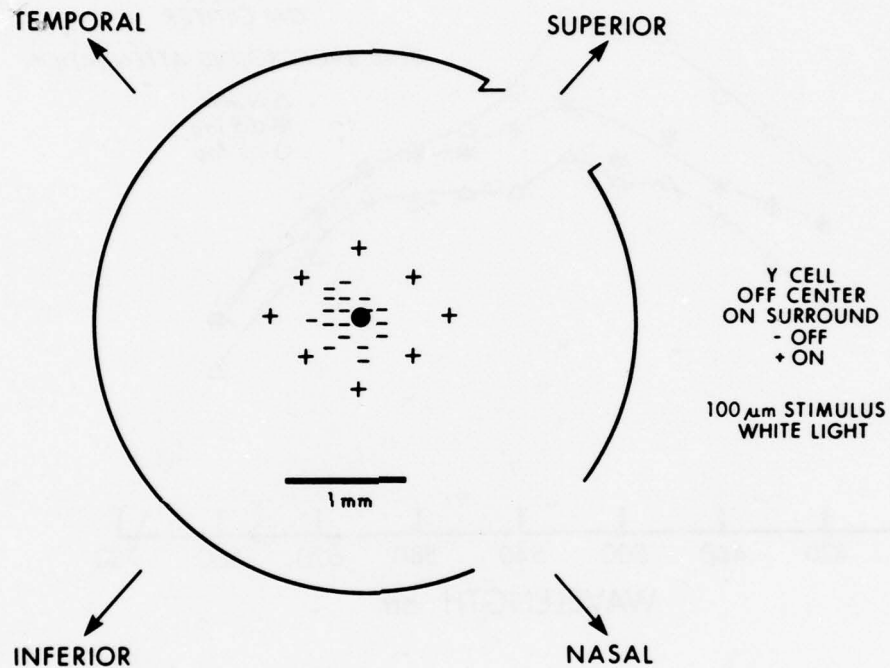
32

Figure 16. A receptive-field plot for a Y cell with off-center/on-surround. The location of the field within the eye in relation to the animal's body is shown. This is a centrally placed cell in the retina, approximately on the optical axis. The test stimulus was a white light, 100-μm spot. The heavy bar indicates 1 mm on the retina to give the actual size of the field.

33
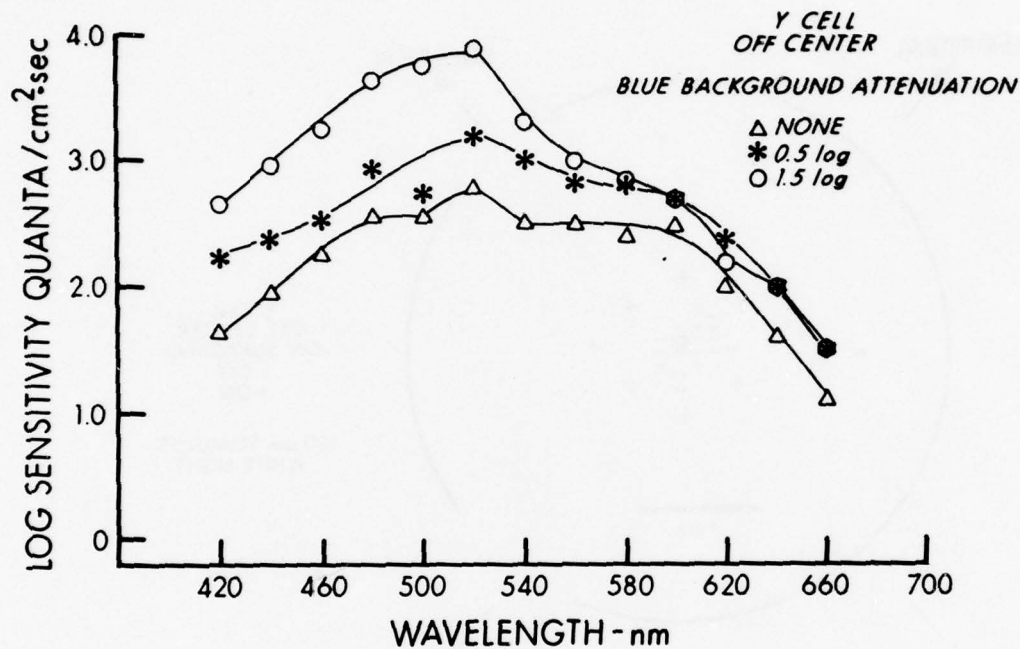
Figure 17. Effects of light adaptation on spectral response. These recordings were made in the presence of a blue background (Wratten #47A). When the background decreases in intensity, the contribution from the short-wavelength end of the spectrum increases, whereas the long-wavelength end of the curve remains fairly constant. The contribution from the short-wavelength end is from a cone system whose sensitivity peak is near 500 nm. The background intensity equals 6.6×10^{13} quanta/cm$^2 \cdot$sec (2.7 µW/cm^2 at 500 nm) on the retina; zero log units in the sensitivity scale equals 3.5×10^{14} quanta/cm$^2 \cdot$ sec (15.1 µW/cm^2 at 500 nm). The stimulus on the retina is 400 µm in diameter. The on-surround response of this cell is shown in Fig. 18.
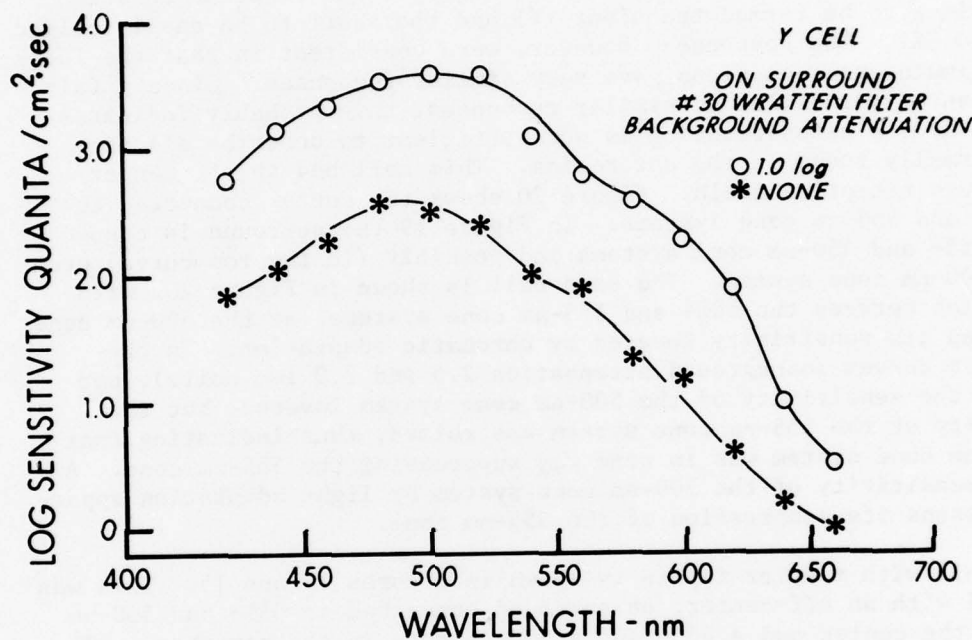
Figure 18. Spectral sensitivity of surround response in a Y cell. The surround shows evidence of both 500- and 555-nm cone processes. The adapting background is a Wratten #30 red filter which peaks at 500-555 nm. This seems to block both cones somewhat, although the long-wavelength end of the spectrum is depressed less than the short-wavelength end. Zero log units on the sensitivity scale equals 3.5 x 10^{14} quanta/cm^2·sec (15.1 μW/cm^2 at 500 nm) on the retina; zero log units in the background equals 4.1 x 10^{13} quanta/cm^2·sec (13.3 μW/cm^2). The surround process is stimulated with an annulus of 1.25-mm inner diameter and 3.0-mm outer diameter. The off-center response of this cell is shown in Fig. 17.

The various cone systems appeared to interact when found in the same part of the receptive field. For example, the cell whose response properties are shown in Figures 19-21 was located on the margin of the area centralis. The responses of this cell did not clearly place it in either the X or Y category. The time constant of any single nerve impulse was too rapid to allow a W classification. The responses had a shorter latency than the sluggish X cells, yet were consistently longer than those cells usually put in the Y category. The response duration was too long to be termed transient (Y) and too short to be easily called sustained (X). The responses, however, were consistent in that the identical stimulus presentations gave very similar responses. Since a fair proportion of our cells had similar responses, this probably indicates that the X, Y, W classification is not sufficient to describe all the cells normally found in the cat retina. This cell had an off center/ on surround receptive field. Figure 20 shows the center connected to the 500- and 555-nm cone systems. In Figure 19 the surround is connected to 555- and 450-nm cone systems and possibly (in the top curve) even to the 500-nm cone system. The same cell is shown in Figure 20, with interaction between the 500- and 555-nm cone systems, as the 500-nm cone system had its sensitivity lowered by chromatic adaptation. In the middle two curves (background attenuation 2.5 and 2.0 log units), not only was the sensitivity of the 500-nm cone system lowered, but the sensitivity of the 555-nm cone system was raised, thus indicating that the 500-nm cone system was in some way suppressing the 555-nm cone. A loss of sensitivity of the 500-nm cone system by light adaptation apparently lessens its suppression of the 555-nm cone.

A cell with simpler inputs is shown in Figures 14 and 15. This was an X cell with an off-center, on-surround connected to 555- and 500-nm cones in the center and a 450- and a 500-nm cone in the periphery. The on response had a fairly long latency; the off response had a rather broad spectral sensitivity. In Figure 15, chromatic adaptation from background lighting was used to lower the sensitivity of the red portion of the spectrum to show more clearly the contribution of the 500-nm cone system mechanism. This cell also had contributions from the rod system as shown by the dark-adaptation curve in Figure 22 in which there is a cone-rod break at approximately 20 minutes. A similar dark-adaptation curve for a Y cell is shown in Figure 7, indicating that both X and Y cells are connected to rods as well as cones.

DISCUSSION

Our results bring out the problems of trying to characterize retinal ganglion cells by examining any single parameter, such as linearity or nonlinearity of responses, shape of receptive field, spectral distribution of the rods and cones connected to it, and receptive-field organization in terms of center/surround. Intense light adaptation of any one of the cone inputs or the rod input could affect all of these parameters, but in ways unpredictable at the present time. Classifying the ganglion cells by

36
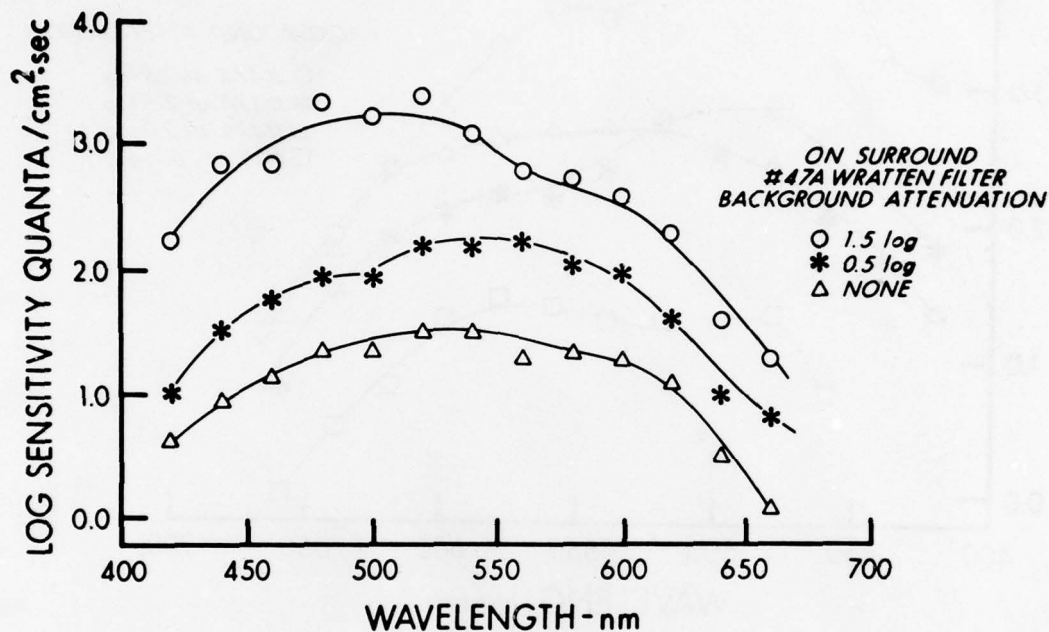
Figure 19. A spectral sensitivity of the on response of an off-center/
on-surround cell. The cell did not clearly fit X or Y classifica-
tion. Adaptation with a blue background depresses the short-
wavelength end of the curve. As the blue background is attenuated,
more contributions from the shorter wavelength end appear. The test
stimulus is an annulus of 1.35-mm inner diameter and 3.00-mm outer
diameter on the retina. Zero log units on the sensitivity scale
equals 5.5×10^{13} quanta/cm^2·sec (2.39 µW/cm^2 at 500 nm) on the
retina; zero log units for the background equals 2.0×10^{12} quanta/
cm^2·sec (0.91 µW/cm^2). Other characteristics of this cell are shown
in Figs. 20 and 21.

Figure 20. Spectral sensitivity of an off response from an off-center/
on-surround cell. This cell did not clearly fit an X or Y classifi-
cation. A blue background markedly decreases the response of the
short-wavelength end of the spectrum relative to the long-wavelength
end. The test stimulus was 200 μm in diameter on the retina. Zero
log units on the sensitivity scale equals 3.5×10^{14} quanta/cm^2·sec
(15.1 μW/cm^2 at 500 nm) on the retina; zero log units for the back-
ground equals 2.0×10^{14} quanta/cm^2·sec (80 μW/cm^2) for the 47A
Wratten filter and 2.0×10^{15} quanta/cm^2·sec (650 μW/cm^2) for the
#15 Wratten filter. Other characteristics of this cell are shown
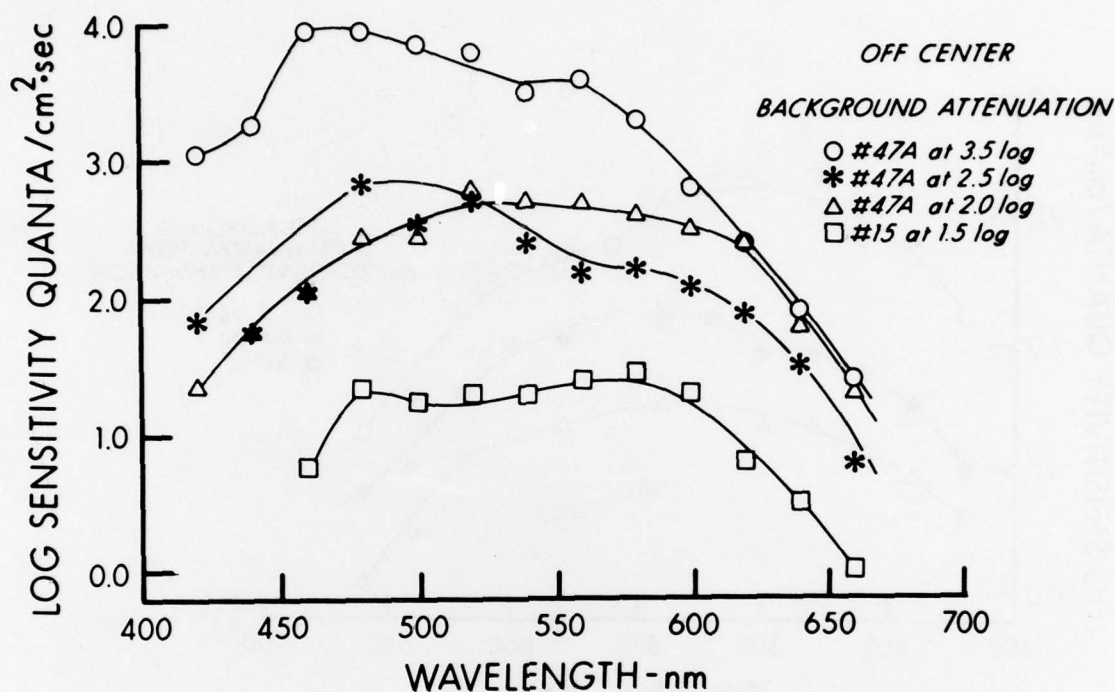in Figs. 19 and 21.
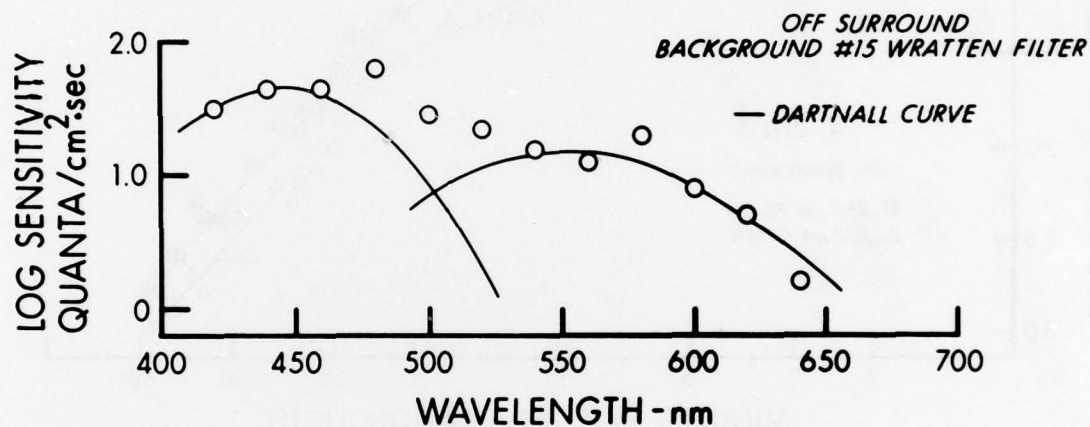
Figure 21. Spectral sensitivity of the peripheral response for an on-
center/off-surround cell. This cell did not clearly fit an X or Y
classification. The test stimulus was an annulus of 1.35-mm inner
diameter, 3.0-mm outer diameter, on the retina. A green background
shows contributions from two cones, 450 and 555 nm; they are com-
pared to Dartnall's nomogram curves with these maximums. The
increased sensitivity at 490 nm is probably an addition of the two
sensitivities. Zero log units on the sensitivity scale equals
3.5×10^{14} quanta/cm^2·sec (15.1 µW/cm^2 at 500 nm) on the retina;
the background equals 6.6×10^{13} quanta/cm^2·sec (20.6 µW/cm^2).
Other characteristics of this cell are shown in Figs. 19 and 20.
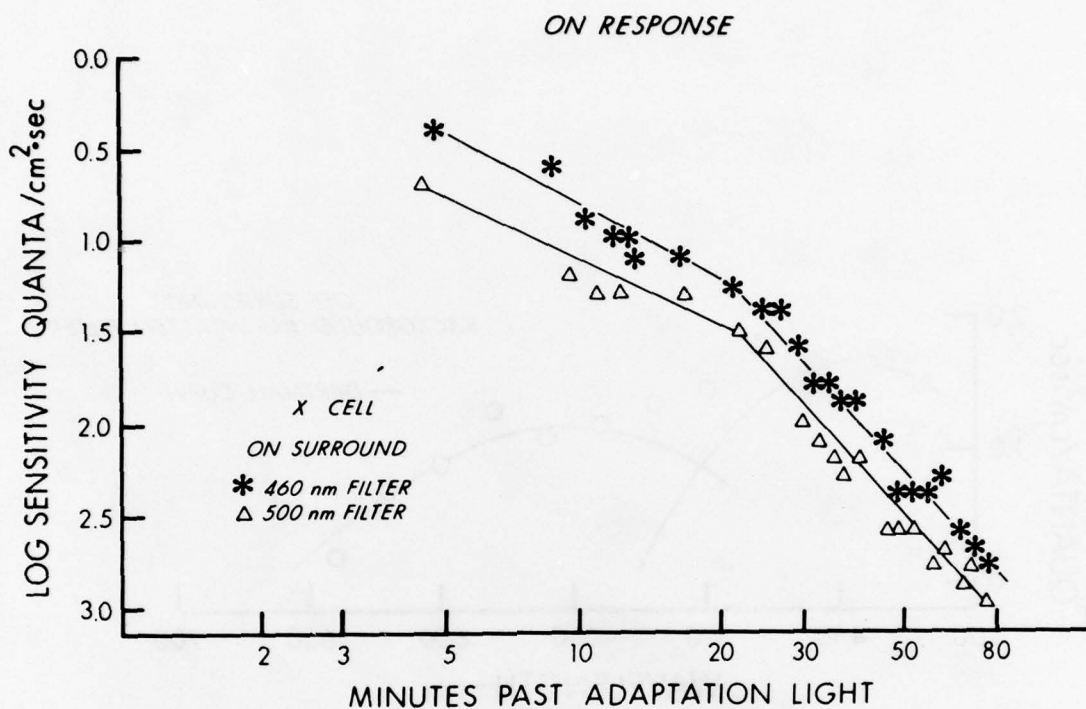
Figure 22. Dark adaptation of the surround response of an X cell off-center/on-surround. The test stimulus was an annulus of 1.35-mm inner diameter and 3.0-mm outer diameter on the retina. The cell was adapted with a Wratten #30 filter for approximately 1 hour. The intensity for the last 15 min was 2.6×10^{14} quanta/cm$^2 \cdot$sec (8.0 μW/cm^2) on the retina, attenuated by 0.7 log units. Zero log units on the sensitivity scale equals 1.1×10^{15} quanta/cm$^2 \cdot$sec (41 μW/cm^2 for 460-nm filter; 48 μW/cm^2 for 500-nm filter). The rod-cone break occurs at approximately 20 min, although it may not be the same for both curves. The spectral sensitivity of the surround in this cell is shown in Fig. 15, and the center is shown in Fig. 14.

40

examining all of these parameters is difficult but not impossible. On the basis of this work and a review of the literature, we suggest that many of the present schemes to classify both cat and monkey retinal cells have different names for identical categories. That is, X, Y, and W cells in the cat retina can be identified with similar cells in the monkey retina. Previous studies (12, 14, 15) suggested that the lack of color-discriminating pathways in the cat retina made it difficult to use as a model for showing functional changes in monkey retinal ganglion cells. Our work suggests that the many reports of qualitative differences between the cat and monkey retina in regard to color-discriminating processes are due perhaps to both quantitative differences and experimental design. The mechanisms for color discrimination in the monkey retina and in monkey behavior are more strongly developed than in the cat, but it still seems reasonable that the same mechanisms are present in the cat, albeit to a lesser degree. The receptive fields appear to be somewhat smaller in the central part of the cat retina than in the periphery. The organization of receptive fields into center and surround, with contributions from cones of either excitatory or inhibitory nature, is not clearly defined. This organization is important to information processing by higher centers, but the available data do not make it possible to suggest any overall principles to aid with the classification of cell types.

One important observation from our data regards cone function. Harwerth and Sperling (30) reported that monkeys can be made insensitive to blue light by chronic exposure to high-intensity blue light, although intense adaptation in other parts of the spectrum produced no corresponding permanent functional disturbances. This indicates some special sensitivity to damage of the mechanism discriminating the blue end of the spectrum; e.g., the blue cones (maximum sensitivity 450 nm), or such intermediate sites as bipolars and horizontal cells, or the synaptic connections to the ganglion cells. No such special lability of the blue-cone system has been seen in the cat nor reported in the monkey ganglion cells. Earlier work on the goldfish retina (14, 47) indicated that the blue system was extremely labile and rarely recovered from intense light exposure; indeed, the blue system often seemed to fade away without any unusual light adaptation. This indicated some difference in function between the blue cones and other types, but the reason for the difference is unknown. It may be an important part of the physiology of the retina, or it may be due to the particular experimental conditions.

The photoreceptors' dependence on vitamin A in the diet has been demonstrated often regarding the rods (41). Cones may similarly be sensitive, and other diet elements such as essential fatty acids might play a role. The work of Noell (41), demonstrating the elevated sensitivity of the rat retina to ambient light levels, indicates that species differences may also be important in this respect. Action of dietary factors on the usual laboratory animals has not been systematically examined in relation to electrophysiological experiments on dark adaptation, so some systematic error in animal maintenance could possibly prove

41

to be an important factor. The experience of Noell (41) in finding his laboratory rats blinded by continuous light at moderate intensities must at least serve as a note of caution in interpreting any changes in function after light adaptation.

At least two components to any change following light exposure must be distinguished. One component may be due to overstimulation of the physiological mechanisms producing normal light adaptation. The first component includes photopigment depletion, depletion of synaptic vesicles, or excessive hyper- or depolarization of a cell in the retinal chain for excessively long periods of time. All of these are exaggerations of the normal accompaniments of ordinary light adaptation. If the light is more intense or maintained for a longer period of time, such mechanisms may be overdriven to the point that the cell is actually damaged or that metabolic support processes in the cell are so depleted that recovery is not possible. The second component includes such factors as excessive heat or thermally enhanced damage to other structural components or metabolic processes. These mechanisms are not normally operative to any significant degree during light adaptation. They must be distinguished as playing a role in damage but not in normal function. Some examples of thermally enhanced photodegradation are the effects on the flavenoid proteins, especially riboflavin. This is found in the pigment epithelium, and its photodegradation there could in turn affect the retina, particularly the 450-nm cones. Photodegradation of the macular pigment is another example, which could also be coupled to damage from blue light such as found by Ham et al. (29) and Harwerth and Sperling (30).

This 450-nm cone system sensitivity to damage has not, however, been found in the cat. This may be a species difference or may indicate that the loss of function is cortical rather than retinal.

Identifying photoreceptor functions from ganglion-cell response curves is not always easy, especially when the ganglion-cell response is made up of perhaps nonlinear combinations of several photoreceptor response functions. Several assumptions are usually made; some appear to be justified, while others are debatable. The first assumption is that the output of the photoreceptor, be it rod or cone, is a linear function of the absorption spectrum of the photopigment in that receptor, at least in the visible range. The absorption and the action spectra may not completely match, however, if inactivated or bleached byproducts of photostimulation themselves absorb in the visible range. The photoproducts of rhodopsin have a low absorption in the visible range after bleaching. For the types of data that we have, the presence of photoproducts would represent only a second-order correction.

The second assumption is that the output of the photoreceptor is represented in the ganglion-cell response by a linear transformation. Under most conditions this assumption is not justified, as many nonlinear transformations can be detected at the ganglion-cell level in the interplay between excitation and inhibition. Even such parameters as latency

42

of response and frequency-dependence of pulsed stimulation, as well as variations of response with intensity, are included. No matter which parameter is used, the same problem exists.

In order to determine whether these assumptions are justified, the results of inferring the photoreceptor response curve from the ganglion-cell response curve are compared with the known details about rod and cone photopigment absorption curves. The most widely accepted way of doing this is to compare the curve derived from the ganglion-cell response with Dartnall's nomogram (11) which assumes that all photopigments, regardless of the λ_{max}, are invariant on a wave number plot (i.e., when the abscissa is reciprocal wavelength). Dartnall's nomogram supplies the details to replot this curve on a wavelength abscissa as a function of λ_{max}. If a supposed receptor curve derived from ganglion-cell data fits a Dartnall curve nomogram of the same λ_{max}, this is deemed sufficient reason to assume linearity in the retina under the particular experimental conditions. The input from the 450-nm cone system shown in Figure 8 is slightly broader than Dartnall's nomogram; however, this deviation is in the direction proposed by Wolbarsht and Yamanashi (60), and thus the curve is probably an accurate representation of the blue-cone response.

The Dartnall nomogram only applies to photopigments whose peak absorption is around 500 nm. Photopigments with peak sensitivity at a shorter wavelength will show spectral sensitivity curves broader than the Dartnall nomogram, while those with peak sensitivity in the red end of the spectrum will have narrower spectral sensitivity curves. At the extreme ends of the spectrum (below 440 nm and above 580 nm) the deviation is large enough to require using a different template when calculating how complex spectral response curves could be formed from interactions of several cone systems. In spite of this systematic deviation from Dartnall's nomogram for all vertebrate photopigments (60), within the wavelength range of 445-565 nm, the deviations, though apparent, are small. Thus, the analysis of the ganglion-cell responses from cat or monkey into inputs from various cone and rod systems should, as a first requirement, approximate Dartnall's nomogram for the various photopigments.

A constant-response-criterion type of experimental design is used to justify the assumption that the ganglion-cell response is a linear function of the photoreceptor response. In our experiments, the stimulus intensity at each wavelength is changed so that the ganglion cell gives the same response relative to some selected criterion point, usually the most sensitive point, or λ_{max}. This can easily be located and used as a criterion. Where there is interaction with other cone systems, some experimental technique must isolate the desired parameter of the response from the influence of other types of inputs. Spatial isolation and chromatic adaptation are frequently but not exclusively employed to this end. Often either the on or off response can be separated so that only one is held constant.

43

Experiments to find dark-adaptation curves that show changes of receptor function must be carefully planned to avoid misleading conclusions. In Figure 7 the two dark-adaptation curves show shifts from rods to cones that differ by almost 25 minutes, depending on the wavelength of the stimulus. This does not indicate a difference in function. The selection of the stimulus can move the curve from one place to the other; i.e., if the cones are stimulated relatively more than the rods with a deep-red stimulus (for the rod sensitivity at the long-wavelength end of the spectrum is very low), then the cones stay more sensitive than the rods for a correspondingly longer period of time and the shift occurs late. This is especially marked because cone sensitivity changes little, and rod sensitivity much. In the dark-adaptation plots, the cone sensitivity quickly reaches a value from which any further adaptation is very slow, perhaps less than a log unit. The rods, during the same period of time, would change 4 to 5 log units. This shows that the rods are much more sensitive to light adaptation and go through a greater range of adaptation. Perhaps their reliable sensitivity to extremely low light levels, even to a single photon, is a consequence of their anatomical and physiological modifications. Although cones respond to a single photon, their responses in that range may not be reliable and may even be ignored by higher order neurons. An extended discussion of this point is not necessary here. It does not seem to be related to the organization of the retina for color discrimination, or form discrimination at photopic levels, but rather is concerned with the reliable detection of signals at scotopic levels, especially at the very-low-light-level end of the scale. The chief interest of this program was the photopic function of the retina, especially toward macular and even foveal organization.

CONCLUSIONS

The present electrophysiological and ancillary techniques are sufficiently stable over long recording sessions to show changes in retinal ganglion-cell characteristics. The types of ganglion cells may be simpler than first proposed. The evidence indicates a general mammalian plan for the retina, with special quantitative modifications for the cat and monkey to suit their particular needs. We conclude that many experiments on cat retinal ganglion cells have a high probability of providing ready assistance with interpretation of similar experiments in the monkey. Both animals have trichromatic color-discriminating mechanisms at photopic levels. Their receptive-field organization of the ganglion cells appears to be similar, although functional changes after intense adaptation have not been completely characterized. The data indicate that the blue-sensitive mechanism at the retinal levels is not necessarily extremely labile as compared with other color processes. This includes both 450-nm cones and retinal pathways associated with them. Recording from single ganglion cells for 10 hours or more allows several dark-adaptation curves to be plotted so that each cell can act

as its own control for intense stimulation. Recordings can be made from preselected parts of the retina with a sufficiently high prospect of success to indicate that the monkey macular region, including the fovea, can be studied extensively and in great detail.

BIBLIOGRAPHY

1. Barnes, F. S. Biological damage resulting from thermal pulses. In M. L. Wolbarsht (ed.). Laser applications in medicine and biology, Vol. 2, pp. 205-222. New York: Plenum Press, 1974.

2. Battista, S. P., and J. M. Davies. Use of electroretinography in the study of flash blindness in animals. In J. M. Davies and D. T. Randolph (eds.). Proceedings of the U.S. Army Natick Laboratories Flash Blindness Symposium, pp. 6-27. Nov 8-9, 1967.

3. Brown, J. L. Experimental investigations of flash blindness. Human Factors 6:503 (1964).

4. Brown, W. E., et al. Anaesthetic value of N_2O under pressure. J Pharmacol Exp Ther 31:269 (1927).

5. Bruce, R., and M. L. Wolbarsht. A system for simultaneously recording from several neurons. Trans BME IRE (In press).

6. Chisum, G. T. Recent research in flash blindness with human subjects. In J. M. Davies and D. T. Randolph (eds.). Proceedings of the U.S. Army Natick Laboratories Flash Blindness Symposium, pp. 54-77. Nov 8-9, 1967.

7. Chisum, G. T. Intraocular effects of flashblindness. Aerosp Med 39(2):860 (1968).

8. Chisum, G. T. Flashblindness recovery following exposure to constant energy adapting flashes. Aerosp Med 44(1):407 (1973).

9. Cleary, S. F. Laser pulses and the generation of acoustic transients in biological material. In M. L. Wolbarsht (ed.). Laser applications in medicine and biology, Vol. 3, pp. 175-219. New York: Plenum Press, 1977.

10. Cleland, B. G., et al. Sustained and transient neurones in the cat's retina and lateral geniculate nucleus. J Physiol 217:473 (1971).

11. Dartnall, H. J. A. The interpretation of spectral sensitivity curves. Br Med Bull 9:24 (1953).

12. Daw, N. W., and A. L. Pearlman. Cat colour vision: evidence for more than one cone process. J Physiol 211:125 (1970).

13. Daw, N. W., and A. L. Pearlman. Rod saturation in the cat. Vision Res 11:1361 (1971).

14. Daw, N. W. Color-coded cells in goldfish, cat, and rhesus monkey. Invest Ophthalmol 11:411 (1972).

15. Daw, N. W. Neurophysiology of color vision. Physiol Rev 53:571 (1973).

16. DeMonasterio, F. M., and P. Gouras. Functional properties of ganglion cells of the rhesus monkey retina. J Physiol 251:167 (1975).

17. DeMonasterio, F. M., et al. Trichromatic colour opponency in ganglion cells of the rhesus monkey retina. J Physiol 251:197 (1975a).

18. DeMonasterio, F. M., et al. Concealed colour opponency in ganglion cells of the rhesus monkey retina. J Physiol 251:217 (1975b).

19. Dow, B. M. Functional classes of cells and their laminar distribution in monkey visual cortex. J Neurophysiol 37:927 (1974).

20. Dow, B. M., and P. Gouras. Color and spatial specificity of single units in rhesus monkey foveal striate cortex. J Neurophysiol 36:79 (1973).

21. Dowling, J. E., et al. Synapses of horizontal cells in rabbit and cat retinas. Science 153:1639 (1966).

22. Enroth-Cugell, C., and J. G. Robson. The contrast sensitivity of retinal ganglion cells of the cat. J Physiol (Lond) 187:517 (1966).

23. Enroth-Cugell, C., and L. H. Pinto. Gallamine triethiodide (Flaxedil) and cat retinal ganglion cell responses. J Physiol 208:677 (1970).

24. Fukuda, Y., and J. Stone. Retinal distribution and central projections of y-, x-, and w-cells of the cat's retina. J Neurophysiol 37:749 (1974).

25. Gibbons, W. D., and R. G. Allen. Evaluation of retinal damage produced by long-term exposure to laser radiation. SAM-TR-75-11, Apr 1975.

26. Granit, R. The antagonism between the on and off systems in the cat's retina. L'Anne Psychol 50:129 (1951).

27. Ham, W. T., Jr., et al. Effects of laser radiation on the mammalian eye. Trans. NY Acad Sci 28:517 (1966).

28. Ham, W. T., Jr., et al. Retinal sensitivity to damage from short-wavelength light. Nature 260:153 (1976).

29. Ham, W. T., Jr. et al. Retinal sensitivity to damage from short-wavelength light. In DeW. G. Hazzard (ed.). Symposium on Biological Effects and Measurement of Light Sources, pp. 37-46. HEW Publication (FDA) 77-8002, 1976.

30. Harwerth, R. S., and H. G. Sperling. Prolonged color blindness induced by intense spectral lights in rhesus monkeys. Science 174:520 (1971).

31. Hayes, J. R., and M. L. Wolbarsht. Thermal model for retinal damage induced by pulsed lasers. Aerosp Med 39(1):474 (1968).

32. Hempel, F. G. Rabbit visual potential after laser photocoagulation. Invest Ophthalmol 10:639 (1971).

33. Hempel, F. G., and A. J. Welch. Evoked potentials from the laser irradiated retina. TR-83, Electronics Research Center, University of Texas, Austin, Tex., Mar 1970.

34. Jones, A. E. Flash blindness experiments with animals: electro-retinographic and behavioral studies. In J. M. Davies and D. T. Randolph (eds.). Proceedings of the U.S. Army Natick Laboratories Flash Blindness Symposium, pp. 138-163. Nov 8-9, 1967.

35. Kozak, W. M., and H. J. Reitboeck. Color-dependent distribution of spikes in single optic tract fibers of the cat. Vision Res 14:405 (1974).

36. Kozak, W. M., et al. Responses of single units in lateral geniculate nucleus of cat to moving visual patterns. J Neurophysiol 28:19 (1965).

37. Levick, W. R. Another tungsten microelectrode. Med Biol Eng 10:510 (1972).

38. MacNichol, E. F., Jr., and T. Bickard. The use of transistors in physiological amplifier. IRE Trans Med Electron PGME 10:15 (1958).

39. MacNichol, E. F., Jr., and J. A. H. Jacobs. Electronic device for measuring reciprocal time intervals. Rev Sci Inst 26:1176 (1955).

40. Mainster, M. A., et al. Retinal temperature increases produced by intense light sources. J Opt Soc Am 60:264 (1970).

41. Noell, W. K., and R. Albrecht. Irreversible effects of visible light on the retina; role of vitamin A. Science 172:76 (1971).

42. Parker, J. F., Jr. Visual impairment from exposure to high intensity light sources. BioTechnology, Inc. Report No. 63-2, May 1963.

43. Pearlman, A. L., and N. W. Daw. Opponent color cells in the cat lateral geniculate nucleus. Science 167:84 (1970).

44. Pitts, D. G. LGN single cell responses as a function of intense light flashes. In J. M. Davies and D. T. Randolph (eds.). Proceedings of the U.S. Army Natick Laboratories Flash Blindness Symposium, pp. 92-119. Nov 8-9, 1967.

45. Priebe, L. A., and A. J. Welch. Changes in the rabbit electro-retinogram c-wave following ruby laser insult. Aerosp Med 44(11):1246 (1973).

46. Randolph, D. I. Electroretinographic and behavioral recovery time of cats to high intensity photopic stimulation. In J. M. Davies and D. T. Randolph (eds.). Proceedings of the U.S. Army Natick Laboratories Flash Blindness Symposium, pp. 164-185, Nov 8-9, 1967.

47. Spekreijse, H., et al. The spectral and spatial coding of ganglion cell responses in goldfish retina. J Neurophysiol 35:73 (1972).

48. Sperling, H. G. Symposium on Biological Effects and Measurements of Light Sources, pp. 47-60. HEW Publication (FDA) 77-8002, Mar 25-26, 1976.

49. Stone, J. A quantitative analysis of the distribution of ganglion cells in the cat's retina. J Comp Neurol 124:337 (1965).

50. Stone, J. Sampling properties of microelectrodes assessed in the cat's retina. J Neurophysiol 36:1071 (1973).

51. Taboada, J., and R. W. Ebbers. Ocular tissue damage due to ultra-short 1060-nm light pulses from a mode-locked Nd:glass laser. Appl Optics 14:1759 (1975).

52. Van Norren, D., and P. Padmos. Influence of anesthetics ethyl alcohol and freon on dark adaptation of monkey cone ERG. Invest Ophthalmol 16:80 (1977).

53. Vassiliadis, A., et al. Investigation of retinal damage using a
    q-switched ruby laser. Stanford Research Institute, Menlo Park,
    Calif. (AD 489376) Aug 1966.

54. Venes, J. L., et al. Nitrous oxide: an anesthetic for experiments
    in cats. Am J Physiol 220:2028 (1971).

55. Vos, J. J. A theory of retinal burns. Bull Math Biophys 24:115
    (1962).

56. Wagner, H. G., et al. The response properties of single ganglion
    cells in the goldfish retina. J Gen Physiol 43(6) (Suppl):45
    (1960).

57. Wagner, H. G., et al. Functional basis for "on" center and "off"
    center receptive fields in the retina. J Opt Soc Am 53:66
    (1963).

58. Wangemann, R. Personal communication, Army Environmental Health
    Agency, Edgewood Arsenal, 1975.

59. Wolbarsht, M. L., and D. H. Sliney. The formulation of protection
    standards for lasers. In M. L. Wolbarsht (ed.). Laser appli-
    cations in medicine and biology, Vol. 2, pp. 309-359. New York:
    Plenum Press, 1974.

60. Wolbarsht, M. L., and B. S. Yamanashi. Chromophore-protein linkage
    and the bathychromic shift in visual pigments. Association for
    Research in Vision and Ophthalmology, Abstracts of Annual Meeting,
    p. 72, #10, 1975.

61. Wolf, E. Early research and physiological implications of flash
    blindness. In J. M. Davies and D. T. Randolph (eds.). Proceed-
    ings of the U.S. Army Natick Laboratories Flash Blindness
    Symposium, pp. 6-27. Nov 8-9, 1967.

62. Zwick, H., et al. Spectral and visual deficits associated with
    laser irradiation. Mod Probl Ophthalmol 13:299 (1974).